

THE RIEMANNIAN STRUCTURE OF EUCLIDEAN SHAPE SPACES: A NOVEL ENVIRONMENT FOR STATISTICS

BY HUILING LE AND DAVID G. KENDALL

University of Nottingham and University of Cambridge

The Riemannian metric structure of the shape space Σ_m^k for k labelled points in \mathbb{R}^m was given by Kendall for the atypically simple situations in which $m = 1$ or 2 and $k \geq 2$. Here we deal with the general case ($m \geq 1$, $k \geq 2$) by using the properties of Riemannian submersions and warped products as studied by O'Neill. The approach is via the associated size-and-shape space that is the warped product of the shape space and the half-line \mathbb{R}_+ (carrying size), the warping function being equal to the square of the size. When combined with parallel studies by Le of the corresponding global geodesic geometry, the results obtained here determine the environment in which shape-statistical calculations have to be acted out. Finally three different applications are discussed that illustrate the theory and its use in practice.

1. Advice to the reader. A palaeontologist comes into your office with a bag of fossils and asks you to devise a natural measure of the difference in shape between any two fossil specimens of a particular genus, with a view to using this in some data-analytic program such as correspondence analysis or nonmetric multidimensional scaling.

An archaeologist asks for your help in assessing the significance of observed “collinearities” of standing stones.

An astronomer trying to match the observed system of cosmic “voids” with the cells of a Voronoi tessellation in three dimensions asks you to help him to classify the sizes and shapes of such cells in sample tessellations generated by a homogeneous three-dimensional Poisson point process.

All these people are asking questions about *shape*. It is not appropriate, however, to think of shapes as points in a Euclidean space. They are odd creatures, and live in peculiar and quite particular spaces most of which occur in no other context. Thus what is required is a revised version of multidimensional statistics that takes the nature of the *shape space* fully into account.

Shape theory was introduced and the very simplest shape spaces fully identified fifteen years ago (Kendall [24]). The present paper identifies the local Riemannian metric geometry of *all* (Euclidean) shape spaces. This is not an easy task. Obviously it involves differential geometry, and that of the most modern sort, because it turns out that what are called *Riemannian submersions* are of fundamental importance in such problems. Riemannian submer-

Received April 1991; revised May 1992.

AMS 1991 subject classifications. Primary 60D05, 62H99.

Key words and phrases. Shape space, Riemannian submersion, warped product, curvature, volume element, singular values decomposition, Brownian motion, shapes of fossils, stereo plots, collinearity testing, Poisson–Delaunay simplexes.

sions were so named by O'Neill [54], but are scarcely ever mentioned in the textbooks, except for O'Neill [56] and Gallot, Hulin and Lafontaine [12]. The first reference to such objects seem to be in Reinhart [57] and Hermann [17, 18]. Thus, while the operations in this paper are "standard" to a modern professional, they involve concepts and constructions normally quite unfamiliar to a mathematical statistician. Because of this the calculations presented here are inevitably taxing, but they are necessary and cannot be circumvented.

In Sections 2 and 3 of the paper we present the basic ideas, and thereafter the pace gets hotter. The reader may reasonably decide to look at those two sections first, and then to pass on at once to the closing Section 8 in which several examples are investigated. These will illustrate what the subject is about, and where it is going.

Further detail can then be sought in the intermediate Sections 4 to 7, where the basic Theorems 1 to 6 and their corollaries are proved. Some rather tricky but necessary analysis occupies Section 4, and perhaps only the most dedicated will wish to read that in detail.

2. Introductory remarks. "Shape" for us means "what is left when the effects associated with translation, scaling and rotation are filtered away" (Kendall [24]). Weaker concepts of shape are also of interest, but will not be treated here. One such is "affine shape," studied by Ambartzumian [1]. Another is "combinatorial shape," studied for example by Carne [8] and Kendall ([21–23, 35]). A classic example involving this is the problem of recovering the topographical structure of a manorial estate from archival references to the abutments of field units.

In the present paper the context will always be a Euclidean space \mathbb{R}^m where the dimension m can be any positive integer, and the shape will be determined by the locations of *labelled* points P_1, P_2, \dots, P_k , where $k \geq 2$. "Size" will be defined to be the square root of the sum of the squares of the distances of these points from their centroid, and it is to be scaled to the value 1 when the size is not of interest and only the shape of the k -plet is being considered. "Location" has already been lost by the choice of the centroid as origin, and the effects of "rotation" are to be removed by insisting that this partly standardized configuration be viewed modulo the rotation group $\mathbf{SO}(m)$.

We shall also be concerned with the less severely standardized object called "size-and-shape." This is the object obtained when the size-standardisation step is omitted. It is to be noticed that "size-and-shape" is meaningful when $k = 1$, although "shape" is not.

The Euclidean shape space Σ_m^k is defined to be *the space whose points are the shapes of such labelled (not totally degenerate) k -ads in \mathbb{R}^m* . These spaces were introduced at a meeting on stochastic geometry and geometrical probability held (in honour of Buffon) on the shores of Lake Sevan in Armenia (Kendall [24]), but for a long time their metrical structure was known only in the relatively trivial cases $m = 1$ (when they are spheres of dimension $k - 2$ with unit radius) and $m = 2$ [when they are complex projective spaces with

real dimension $2(k - 2)$ and complex sectional curvature constant 4], so that, for instance, Σ_2^3 is the sphere $\mathbb{S}^2(\frac{1}{2})$.

Shape space theory for $m = 1$ and 2 was expounded in full detail in Kendall [26]. (His paper [27] gives a less technical presentation.) Here our first purpose is to give a comprehensive account of the local Riemannian geometry for all values of k and m .

For a complete understanding of the structure of these spaces we also need global information. Le [49] has recently given a detailed account of the global geodesic geometry of Σ_m^k , with a specification of the cut-locus phenomena (e.g., the "focussing" properties of the geodesic sprays) and of the behaviour of geodesics near to the singularities (which we shall find are always present when the ambient dimension m exceeds 2 and k exceeds 3), while Kendall [36] has found the Z_2 and rational homologies and Barden [3] the integral homology. The description of the Euclidean shape spaces Σ_m^k is thus approaching completion, although some further information concerning their structure as CW-complexes and their homotopy types may shortly be forthcoming.

Le's article [49] was followed by Le [50], which deals with global questions such as the construction of geodesics that start out from a given point and subsequently cut a given submanifold of the shape space orthogonally. *This will be recognised at once as a key step in the transfer of classical linear multivariate ideas to a shape-theoretic context.* An account of its use in a practical problem will be given in Section 8.

A basic feature of our approach will be to start with the size-and-shape space $\mathbf{S}\Sigma_m^k$, and then to construct the shape space Σ_m^k by *quotienting out the size*. That is easy enough to visualise when the ambient dimension $m = 1$, for then, as we shall see, the size-and-shape space is \mathbb{R}^{k-1} and the shape space is the unit sphere of dimension $k - 2$ with centre at the origin.

As an introduction to the later arguments we now describe the construction of Σ_1^k in more detail. Let the given configuration of points be $(x_1^*, x_2^*, \dots, x_k^*)$ with centroid x_c^* , and let us standardize for location by writing $y_i = x_i^* - x_c^*$, so that $\sum y_i = 0$. To standardize also for size we then have to restrict attention to the intersection of that $(k - 1)$ -dimensional hyperplane with the unit sphere centred at the origin in y -space, and obviously this intersection is the unit sphere $\mathbb{S}^{k-2}(1)$, which therefore is Σ_1^k up to isometry. Note, in particular, that Σ_1^2 is the point-pair $\{-1, 1\}$. (This is the only shape space that is not connected.)

The corresponding size-and-shape space $\mathbf{S}\Sigma_1^k$ is obtained if we relax the size restriction, so that it is the whole Euclidean space \mathbb{R}^{k-1} , and we can think of this as an (unwarped) cone with spherical cross section $\mathbb{S}^{k-2}(r)$ at distance r along the generators. In particular $\mathbf{S}\Sigma_1^2$ is just \mathbb{R}^1 viewed as a one-dimensional cone with the point $\{-1, 1\}$ as the cross section at distance $r = 1$. The absence of warping is a way of saying that the radial size of the spherical cross section is everywhere equal to the corresponding radial distance from the vertex.

*But now observe what happens when the ambient dimension $m \geq 2$. The size-and-shape space is then difficult to visualise, although its structure is still basically very simple. Thus when the ambient dimension m is equal to 2 then

the size-and-shape space is a cone with the shape space Σ_2^k of the k -point configuration as the cross section at $r = 1$. However, Σ_2^3 is the (metric) sphere $\mathbb{S}^2(\frac{1}{2})$ (for the simplest proof of this see Kendall [27]). Try to visualise a cone whose cross section at distance r from the vertex is a two-sphere of radius $\frac{1}{2}r$! This illustrates a peculiarity of the size-and-shape spaces $\mathbf{S}\Sigma_2^k$, and that phenomenon is the norm—it is the case $m = 1$ that is the exception. In what follows we shall often prefer to say, for example, that the size-and-shape space $\mathbf{S}\Sigma_2^3$ is the *warped cone* with cross section $\mathbb{S}^2(1)$ and with *warping function* $\frac{1}{4}r^2$, where r is the distance along the axis from the vertex of the cone. To illustrate the terminology we observe that \mathbb{R}^2 with metric $dr^2 + r^2 d\theta^2$ can be described as the warped product of a half line and a unit circle with warping function r^2 . (See O’Neill’s book [56] for other examples of warping.)

We have now dealt exhaustively with the size-and-shape and shape spaces when $m = 1$, and we have shown by an example the peculiarities that are encountered when $m \geq 2$. In particular, as remarked above (see also Kendall [26]), the shape space Σ_2^k is that version of complex projective space $\mathbb{C}\mathbb{P}^{k-2}$ whose linear scale is such that the (constant) sectional curvature is equal to 4. The reader who does not already know that $\Sigma_2^3 = \mathbb{S}^2(\frac{1}{2})$ is urged to look at the elementary but rather lengthy proof of this fact in Kendall [27], and perhaps also at the (yet longer) proof that $\Sigma_2^k = \mathbb{C}\mathbb{P}^{k-2}(4)$ in Kendall [26]. It is an important fact that all of the shape spaces Σ_1^k and Σ_2^k are compact and are free from singularities.

But when we proceed to the shape spaces Σ_m^k with $m \geq 3$ a new phenomenon appears. For $k > m$ each shape space now contains singularities at the differential level. This is a striking new phenomenon because when m is equal to 1 or 2 then each shape space has a transitive group of isometries, so that there “all points are alike” and such shape spaces are then necessarily nonsingular. Thus the jump in ambient dimension from 1 to 2 introduces the peculiar warping of the size-and-shape space, while the jump from 2 to 3 and beyond introduces the differential singularities.

Another discontinuity of behaviour occurs when m increases from $k - 1$ to k . What happens there and for all higher values of m is that the shape spaces acquire *boundaries*. Thus, for example, Σ_2^3 is a two-sphere of radius $\frac{1}{2}$, but Σ_3^3 is homeomorphic with a two-ball, and this is also true of Σ_m^3 for all higher values of m . This phenomenon is typical; for each k it sets in at $m = k$. (In the degenerate case $k = 2$, Σ_1^2 is the point-pair $\{-1, +1\}$ while Σ_m^2 is a *single point* for all $m \geq 2$.)

After reading an earlier draft of this paper a referee suggested that it might help the reader if each new increase in ambient dimension were explicated by reference to the lower ambient dimensions, but that is not in fact a helpful procedure. As so often in geometry, a rise in dimension may (and here in many ways does) lead to totally new types of behaviour. However, there is one partial simplification for high ambient dimensions: Σ_m^k is isometric with Σ_k^k for all $m > k$. Also the reader might here like to glance ahead to the second remark in Section 5, and note the useful *nesting principle* established there.

TABLE 1

$m =$	1	::	2	::	3	4	5	6	7	8
$k = 2$:: * Σ_1^2 *	::	Σ_2^2	::	Σ_3^2	Σ_4^2	Σ_5^2	Σ_6^2	Σ_7^2	Σ_8^2
$k = 3$:: Σ_1^3	::	* Σ_2^3 *	::	Σ_3^3	Σ_4^3	Σ_5^3	Σ_6^3	Σ_7^3	Σ_8^3
$k = 4$:: Σ_1^4	::	Σ_2^4	::	* Σ_3^4 *	Σ_4^4	Σ_5^4	Σ_6^4	Σ_7^4	Σ_8^4
$k = 5$:: Σ_1^5	::	Σ_2^5	::	Σ_3^5	* Σ_4^5 *	Σ_5^5	Σ_6^5	Σ_7^5	Σ_8^5
$k = 6$:: Σ_1^6	::	Σ_2^6	::	Σ_3^6	Σ_4^6	* Σ_5^6 *	Σ_6^6	Σ_7^6	Σ_8^6
$k = 7$:: Σ_1^7	::	Σ_2^7	::	Σ_3^7	Σ_4^7	Σ_5^7	* Σ_6^7 *	Σ_7^7	Σ_8^7
$k = 8$:: Σ_1^8	::	Σ_2^8	::	Σ_3^8	Σ_4^8	Σ_5^8	Σ_6^8	* Σ_7^8 *	Σ_8^8
$k = 9$:: Σ_1^9	::	Σ_2^9	::	Σ_3^9	Σ_4^9	Σ_5^9	Σ_6^9	Σ_7^9	* Σ_8^9 *

We now set out in a two-dimensional array the first few shape spaces, arranged so that the ambient dimension m increases as we move to the right from column to column, while the number k of points increases as we go down the columns. This will bring out more clearly some of the variations of structure on an (m, k) -basis.

Table 1 indicates by colons and asterisks the locations of the spheres $\Sigma_1^k = S^{k-2}(1)$, the complex projective spaces $\Sigma_2^k = \mathbb{C}P^{k-2}(4)$, and the (for $m \geq 3$ nonmetric) spheres Σ_m^{m+1} to the right of which are situated balls (for $m \geq 3$ also nonmetric) all with dimension $\frac{1}{2}k(k-1) - 1$. Notice especially that each space in the row $k = 2$ is a point or a point-pair, while all the spaces in the second row are metric spheres or hemispheres. In the quadrant lying below the second row and to the right of the second column (i.e., when both $k \geq 4$ and $m \geq 3$) each shape space possesses singularities at the differential level. The fact that every shape space on the diagonal $k = m + 1$ is a *topological* sphere was discovered in 1976 by A. J. Casson (unpublished). A later and different proof of that fact given in Le [49] will be outlined here in Section 3.

A thorough familiarity with the above diagram will be very helpful to the reader intending to work through the following arguments, and indeed it is also necessary for a proper understanding of the applications.

An early draft of the present paper was used by Kendall as the basis of his Rietz Lecture to the Institute of Mathematical Statistics at its Annual Meeting in Washington, DC, in 1989. That lecture was largely concerned with the applicable aspects, and indeed much of the detailed metrical theory presented in the present paper was not fully worked out until somewhat later by Le.

Some of what follows may at first sight seem remote from statistics, but it is statistically motivated, and it is the indispensable preliminary to any general approach to shape statistics.

Already (as will be seen in the closing Section 8) the metrical theory developed in the Sections 3 to 7 has found statistical applications, and one cannot doubt that more will follow, especially in the light of recent work by Goodall and Mardia [13-15].

As its title indicates, the present paper deals only with what we call the *Euclidean* shape spaces concerned with the shapes of labelled sets of points in

Euclidean spaces \mathbb{R}^m . The reader is however reminded that there is a companion theory, that of *spherical* shape spaces (Le [45–47]), in which the k labelled points lie on the surface of a two-sphere. This has applications in astronomy. A further extension to shape theory on an m -sphere will be found in Carne [7]. For a gentle initiation into spherical shape-space theory see Kendall [34].

We say nothing in this paper about *shape distributions* because that topic has been covered already in considerable detail. For shape distributions generated by k iid-uniform points in compact convex polygons see Le [43, 44] and Kendall and Le [38, 39], and for those generated by k -point multivariate Gaussian distributions see Mardia and Dryden ([52, 53] and subsequent papers). It is often convenient to present such shape distributions as densities relative to the natural differential-geometric measure on the shape space, and here the second part of Corollary 1 in Section 5 provides an appropriate starting point. Similarly Corollary 3 in the same section links the present paper with Bru [6], W. S. Kendall [40, 41] and Le [51] on shape diffusions. Notice that diffusion theory can be used to obtain some of the Gaussian-based shape-densities. For this see Kendall [32] and Le [48].

3. Size and shape. We now embark on the determination of the local Riemannian geometry for all k and all m . As remarked above, by the “shape” of a set of k labelled points in \mathbb{R}^m we always mean “what is left when the effects associated with translation, rescaling and rotation are filtered away.”

We map the i th point x_i^* of a given set of k labelled points in \mathbb{R}^m to $x_i^* - x_c^*$ in order to eliminate the effects of translation, where x_c^* denotes the centroid of the k points. This converts the original $m \times k$ data matrix X^* to a matrix with zero row-sums. If we multiply this new matrix on the right by Q , where Q is any *fixed* “cosmetic” element of $\mathbf{O}(k)$ such that

$$Q(1, 0, \dots, 0)^t = (1, 1, \dots, 1)^t / \sqrt{k},$$

then the zero-row-sum property will be replaced by that of having a zero first column. We can then delete that column to get an $m \times (k - 1)$ matrix \tilde{X} that will be called the *presize-and-shape* of the k labelled points specified by X^* . The space of all such matrices will be identified with $\mathbb{R}^{m(k-1)}$. Then

$$r = \sqrt{\text{tr}(\tilde{X}^t \tilde{X})} = \sqrt{\text{tr}(\tilde{X} \tilde{X}^t)} = \sqrt{\sum |x_i^* - x_c^*|^2}$$

is a natural measure for the *size* of the set of k points. Accordingly the size-standardized version $X = \tilde{X}/r$ of \tilde{X} will be called the *preshape* of X^* . Note that *presize-and-shape* (*but not preshape*) is well defined when the points are totally coincident, that is, when $r = 0$. It is clear that the preshape space is the sphere $\mathbb{S}^{m(k-1)-1}(1)$. [Here and elsewhere the prefix “pre” indicates that the quotient by $\mathbf{SO}(m)$ has not yet been formed.]

The “cosmetic” matrix Q is not unique, but it is to be fixed in the following analysis. We shall see that neither the multiplication by Q nor the deletion of the zero first column when forming \tilde{X} will have any effect on our final results, because those will be expressed in terms of the eigenvalues of $\tilde{X} \tilde{X}^t$. This

feature of the method therefore spares us the trouble of working with $m \times k$ matrices having an artificial rank-deficiency as a consequence of the centring procedure.

Quotienting out the left action of $\mathbf{SO}(m)$ on $\mathbb{R}^{m(k-1)}$ and on $\mathbb{S}^{m(k-1)-1}(1)$ gives the size-and-shape space $\mathbf{S}\Sigma_m^k$ and the shape space Σ_m^k , respectively. Note in particular that $\mathbf{S}\Sigma_m^2$ is \mathbb{R} for $m = 1$, and \mathbb{R}_+ for $m \geq 2$. Also Σ_1^k is $\mathbb{S}^{k-2}(1)$ for $k \geq 2$, and Σ_2^k is $\mathbb{C}\mathbb{P}^{k-2}(4)$ for $k \geq 3$. [Note also that $\mathbb{C}\mathbb{P}^1(4) = \mathbb{S}^2(\frac{1}{2})$.]

Left multiplication by $\text{diag}(1, \dots, 1, -1)$ on the presize-and-shape space induces an action of \mathbb{Z}_2 on $\mathbf{S}\Sigma_m^k$ (cf. Kendall [26]). (Matrix-wise it switches the algebraic signs in the m th row.) For $m \geq k$, $\mathbf{S}\Sigma_m^k$ and Σ_m^k are isometric with the quotient $\mathbf{S}\Sigma_{k-1}^k/\mathbb{Z}_2$ and $\Sigma_{k-1}^k/\mathbb{Z}_2$, respectively. [It is this \mathbb{Z}_2 -quotient operation that converts the topological spheres on the diagonal of the (k, m) -diagram to the topological balls lying to the right of them.] Therefore in the following calculations we can and often will assume that $k \geq m + 1$.

It will now be convenient to quote from Dieudonné [9] some definitions and theorems concerning the action of a Lie group G acting smoothly on a differential manifold M . (See also Helgason [16].)

(i) (Vol. II, XII.10, Problem 1) The action of G on M is said to be “proper” when, for all compact sets K and L , the set $\{g: (gK) \cap L \neq \emptyset\}$ is compact. The action will always be proper if G is itself compact. In our application that condition will hold because G will be $\mathbf{SO}(m)$.

(ii) (Vol. II, XII.10) The action of G on M is said to be “free” when every g that is distinct from the unit element e leaves no x in M unmoved.

(iii) (Vol. III, XVI.10, Theorem 3 and Problem 1) The orbit manifold M/G exists as a differentiable manifold if the action of G is both proper and free. When it is proper but not everywhere free then M/G exists as a differentiable manifold with singularities at just those x in M at which the action is not free, so that the singularities in the orbit manifold are precisely located at the images of those x such that $gx = x$ for some g other than the identity.

Now in our problem M will be the preshape space X , and G will be the compact Lie group $\mathbf{SO}(m)$. Thus (i) always holds, and (ii) will also hold if the ambient dimension m is equal to 1 or 2, so that Σ_1^k and Σ_2^k are smooth manifolds for all $k \geq 3$. We do not need to worry about the rather trivial cases in which $k = 2$, because we already known that Σ_m^2 is either a point or a point-pair.

When $m \geq 3$, however, singularities always exist, and we can identify them quite easily: They correspond to the preshape matrices of rank $m - 2$ or less. This is because, if X has at most $m - 2$ linearly independent rows, then a nontrivial element of the form

$$R_m^t \text{diag}(I_{m-2}, R_2) R_m$$

with $R_2 (\neq I_2) \in \mathbf{SO}(2)$ and $R_m \in \mathbf{SO}(m)$ can always be found that leaves X invariant. Away from such singularities the action will be both proper and free, but the quotient by $\mathbf{SO}(m)$ will be a noncompact smooth manifold Σ_m^k

whose singularities are determined precisely by the nonfree action of $\mathbf{SO}(m)$. So if we leave aside the cases where $k = 2$, we can conclude that Σ_1^k and Σ_2^k are always smooth, while Σ_m^k (for $m \geq 3$) is smooth *save for just those singularities noted above*.

Moreover in the situation considered here it is known that the quotient mapping π from the preshape space to the shape space is a *Riemannian* submersion and enjoys all the properties of such a mapping *away from just those singularities that we have found*. We here remind the reader that in general a "submersion" is a smooth mapping from a manifold M_1 onto another smooth manifold M_2 such that the rank of the Jacobian is everywhere equal to $\dim M_2$. That we have a submersion in our application follows immediately from (iii) above. However it is the much more special *Riemannian* submersions that play a fundamental role in shape theory. We now give the definition and list some properties of these objects.

First we must introduce the concept of *vertical* and *horizontal* tangent vectors in the "top" space M_1 (for us, the preshape space). A tangent vector at x in the top space is said to be *vertical* if it is tangent to the *fibre* through x . [The fibre is the set $\pi^{-1}(\pi(x))$ of all the preimages of $\pi(x)$.] Tangent vectors at x in the top space that are orthogonal to all the vertical tangent vectors at x are said to be *horizontal*. Thus the tangent space at x in the top space splits into a direct sum: "horizontal tangent vectors \oplus vertical tangent vectors."

The definition of a *Riemannian* submersion can now be given. A submersion from the ("top") Riemannian manifold M_1 onto the "bottom" Riemannian manifold M_2 is said to be *Riemannian* when each pair of horizontal tangent vectors (h_1, h_2) at any $x \in M_1$ maps under $d\pi$ to a pair of tangent vectors at $\pi(x) \in M_2$ that have the same inner product. It is just this metrical condition that makes the theory work.

It is now easy to define a Riemannian metric on the shape space (away from the singularities) in such a way that we do have a Riemannian submersion. Anticipating here a systematic notation to be introduced in Section 4 we write UAV for the singular-values decomposition of a preshape X , so that $U \in \mathbf{SO}(m)$, $V \in \mathbf{SO}(k-1)$ and Λ is an $m \times (k-1)$ -matrix whose first m columns are $\text{diag}(\lambda_1, \lambda_2, \dots, \lambda_{m-1}, \lambda_m)$ where $\lambda_1 \geq \dots \geq \lambda_{m-1} \geq |\lambda_m|$ and whose remaining columns (if there are any) are zero.

The *vertical* tangent vectors (tangents to the fibre) at this point will then be represented by the matrices $\$UAV$ where $\$$ is a general $(m \times m)$ skew-symmetric matrix, and so a tangent vector W at the same point will be *horizontal* if and only if

$$\text{tr}(W\$UAV) = 0$$

for every choice of $\$$, that is, if and only if $UAVW^t$ is symmetric.

Now consider two such horizontal tangent vectors $UAVW_1^t$ and $UAVW_2^t$ at the given point of the top space. Their inner product is $\text{tr}(UAVW_1^t W_2 V^t \Lambda^t U^t)$, and in this expression the first and last factors within the brackets cancel, so that the inner product is just $\text{tr}(\Lambda V W_1^t W_2 V^t \Lambda^t)$, and this no longer depends on the location (indicated by U) on the fibre. This argument therefore establishes

the Riemannian nature of the submersion and so allows us to make use of O'Neill's theorems [54–56].

One of these tells us that locally (i.e., away from the singularities if there are any) the geodesics in the bottom space are the π -images of the *horizontal* geodesics in the top space, and further that a geodesic in the top space that is horizontal at a point x will remain horizontal (i.e., have a horizontal tangent vector) everywhere along its length until and if it hits a singularity. Thus the geodesic field in the bottom (here shape) space can be calculated from the *horizontal* geodesic field in the top (here preshape) space.

The paper by Le [49] carries out exactly that programme. She obtains a complete description of the cut-locus phenomena in Σ_m^k , determining for each geodesic the point at which the cut-locus is first hit, and using this to study the metrical shape-space architecture on a global basis. In particular she obtains a new proof of Casson's theorem that asserts the (in general only topological) spherical nature of Σ_m^{m+1} . Because of its intrinsic interest we give a brief nontechnical outline of her argument. Consider first the special shape ("the north pole") associated with the diagonal matrix each of whose m diagonal entries is equal to $1/\sqrt{m}$. If one follows each one of the geodesics emerging from that point, one can show that it remains minimal and does not hit the cut locus of the north pole at least until the "equator" is reached, and that every point on the equator (regular or not) is so reached. (By "the equator" we here mean the locus of shapes for which the associated $m \times m$ matrix has a zero determinant.) Thus the whole "spray" of geodesics emerging from the north pole determines a (topological) ball "centered" at the north pole and having the equator as its boundary. Moreover the whole of the equator is in the boundary of this ball.

We can now carry out the same construction starting from the "south pole" (the shape representing the matrix $\text{diag}(1/\sqrt{m}, \dots, 1/\sqrt{m}, -1/\sqrt{m})$), and we obtain a second "ball" *having the same boundary as the first ball*. Identification of the two boundaries yields a topological sphere, and that last step essentially concludes the proof. (Casson's argument finishes in the same way, but starts differently, creating the balls by an algebraic rather than a geometric construction.) Of course both arguments work perfectly well when $m = 2$, but the situation there is much simpler because of the absence of singularities.

It will be convenient to say a few words here about the singularity set. We have already indicated earlier in this section that singularities in the shape space arise when and only when we are considering a shape that is the image of a preshape *at which the Lie group [here $\mathbf{SO}(m)$] fails to act freely*. If we consider the left action of $\mathbf{SO}(m)$ on the preshapes, viewed as $m \times (k - 1)$ real matrices with the squares of the elements summing to unity, it will be apparent that the action of $\mathbf{SO}(m)$ will fail to be free *precisely when the $m \times (k - 1)$ matrix has rank $m - 2$ or less*. (Notice that this cannot happen when m is equal to 1 or 2.) Now the rank is itself a well-defined function of shape, and so we can classify all the shapes in a shape space Σ_m^k according to the rank of any one "representing matrix." Consider those shapes in Σ_m^k that

have rank r less than or equal to a fixed value ρ , where $1 \leq \rho \leq m - 2$. Each of these shapes will be singular, from what has been said above. Also the set of shapes for which the rank is ρ or less (for a given ρ that satisfies $1 \leq \rho \leq m - 2$) can be identified with a “projectivised” version of Σ_ρ^k associated with the $\rho \times (k - 1)$ preshape matrices that [modulo $\mathbf{O}(\rho)$] can be arranged to have a nonnegative element terminating every one of the ρ rows.

In this rather limited sense we have a “nesting principle” that up to such projectivisation allows us to recognise “earlier” shape spaces with $m = \rho$ inside “later” shape spaces with $m > \rho$. We shall meet this “nesting principle” again in Section 5, where we write Σ_r^k/\mathbb{Z}_2 for the thus projectivised version. In fact the corresponding result described in the remark at the end of Section 5 appears to be stronger than that claimed here, but this is because the projectivisation leaves the structure of small neighbourhoods unchanged, and so it cannot be detected at the level of the metric tensor alone.

A final and very important theorem of O’Neill [54, 55] tells us how to compute the curvature characteristics of the bottom (shape) space from those of the top (preshape) space. Because the preshape space is a sphere (and as such has trivial curvature properties) this will spare us a huge amount of detailed calculation.

It is important to notice that singularities cannot occur at all in the shape space Σ_m^k when $k \geq 3$ and m is equal to 1 or 2, because if there are no more than two rows in a matrix representing a preshape then obviously its rows cannot be $\mathbf{SO}(2)$ -rotated so as to yield two empty rows. This explains why the shape spaces Σ_1^k (all spheres) and Σ_2^k (all complex projective spaces) are complete manifolds free of singularities when $k \geq 3$.

Note finally that the diagram

$$\begin{array}{ccc} \tilde{X} & \rightarrow & X \\ \downarrow & & \downarrow \\ \pi(\tilde{X}) & \rightarrow & \pi(X) \end{array}$$

is commutative, where the horizontal arrows indicate standardization for size, the vertical arrows indicate the submersive action, and $\pi(\tilde{X})$ denotes a size-and-shape and $\pi(X)$ the corresponding shape.

4. Coordinates, differential forms and vector fields. In this section of the paper we introduce appropriate coordinates for both size-and-shapes and shapes, and develop a number of ideas that will be important later. In particular, we establish a “continuity principle” that will enable us to ignore irrelevant (but otherwise bothersome) degeneracies.

One can set up coordinates for size and shape in various ways. For example the set of coordinates devised and used by W. S. Kendall [40, 41] in his study of shape diffusion is the complete set of interpoint distances, and by using these he obtained an expression for the Riemannian metric structure via the quadratic component of the submersed Laplacian. That system of coordinates is superabundant when $k > m + 1$, but it was used by him to good effect in a

computer-algebra context where overall symmetries supply a vital tool for controlling and ordering the calculation.

Here we describe, in terms of singular-values decompositions of $m \times (k - 1)$ matrices, a local representation for presize-and-shape that can be well defined away from a set of measure zero. This representation will also induce a local representation for the associated size-and-shape space and the shape space. While it is useful to have these coordinates, we will be forced to concentrate on the differential forms and associated vector fields that are needed in the metric, curvature and other tensorial calculations. An old-fashioned “coordinate” approach would be possible but very complicated and inelegant, and out of tune with the general theory of Riemannian submersions on which we will have to call.

It has to be pointed out that there is a limit to the extent to which the higher dimensional calculations can be explicated in terms of those available for small values of m . Once the “elementary” cases $m = 1$ and $m = 2$ have been fully worked out, we have to proceed immediately to the general case. It is at this point that the reader may well prefer to jump ahead to the examples in Section 8 (at any rate in a first reading). In a second reading it will probably prove most convenient to pay particular attention to the special case Σ_3^4 (in which singularities first make their appearance). This might be described as the first “typical” shape space, and as the associated analysis involves nothing worse than 3×3 matrices it is not unduly difficult to comprehend.

In the following calculations we can without loss assume that $k \geq m + 1$ and $m \geq 3$, because the other cases are either already fully understood, or follow easily from these. We can write the presize-and-shape in the form

$$\tilde{X} = U(\tilde{\Lambda} \ 0)V,$$

with $U \in \mathbf{SO}(m)$, $V \in \mathbf{SO}(k - 1)$ and $\tilde{\Lambda} = \text{diag}(\tilde{\lambda}_1, \tilde{\lambda}_2, \dots, \tilde{\lambda}_m)$ such that:

- (i) $\tilde{\lambda}_1 \geq \tilde{\lambda}_2 \geq \dots \geq |\tilde{\lambda}_m| \geq 0$,
- (ii) $\tilde{\lambda}_m \geq 0$ if $k > m + 1$ and $\text{sign}(\tilde{\lambda}_m) = \text{sign}(\det(\tilde{X}))$ if $k = m + 1$.

From the point of view of shape theory U is uninteresting, and the important information is held in $\tilde{\Lambda}$ and V . We need however to keep track of U because that provides the coordinates describing position on the fibre.

In the above “singular-values decomposition” the $|\tilde{\lambda}_i|$'s are the m ordered nonnegative square roots of the eigenvalues of $\tilde{X}\tilde{X}^t$, and so $\tilde{\Lambda}$ is uniquely determined by $\pi(\tilde{X})$. In particular $\sum \tilde{\lambda}_i^2 = r^2$, where r is the size. Hence $\mathbb{S}^{m(k-1)-1}(1)$ consists of points that are the $m \times (k - 1)$ matrices \tilde{X} , and Σ_m^k consists of points that are the $\pi(\tilde{X})$ with $\sum \tilde{\lambda}_i^2 = 1$. Moreover, the singularities associated with the nonfree action of $\mathbf{SO}(m)$ occur precisely when $\tilde{\lambda}_{m-1} = \tilde{\lambda}_m = 0$.

The matrix U can be naturally regarded as a rotation that rearranges the points on the “fibre” lying above $\pi(\tilde{X})$. However, because the columns of U are eigenvectors of $\tilde{X}\tilde{X}^t$ and the rows of V are eigenvectors of $\tilde{X}^t\tilde{X}$ [arranged in the same order as the corresponding eigenvalues $(\tilde{\lambda}_i)^2$], neither U nor V is uniquely determined by \tilde{X} .

We now define two sets involving sharp inequality signs:

$$\mathbb{X}_{m,k} = \begin{cases} \left\{ \tilde{X} \in \mathbb{R}^{m(k-1)} \mid \tilde{\lambda}_1 > \cdots > \tilde{\lambda}_{m-1} > |\tilde{\lambda}_m| \right\}, & \text{if } k = m + 1, \\ \left\{ \tilde{X} \in \mathbb{R}^{m(k-1)} \mid \tilde{\lambda}_1 > \cdots > \tilde{\lambda}_m > 0 \right\}, & \text{if } k > m + 1, \end{cases}$$

and

$$\mathbb{E}^m = \begin{cases} \left\{ x \in \mathbb{R}^m \mid x_1 > \cdots > x_{m-1} > |x_m| \right\}, & \text{if } k = m + 1, \\ \left\{ x \in \mathbb{R}^m \mid x_1 > \cdots > x_m > 0 \right\}, & \text{if } k > m + 1. \end{cases}$$

Note that $\mathbb{X}_{m,k}$ and \mathbb{E}^m have natural differential structures as open subsets of their respective spaces, and that $\pi(\mathbb{X}_{m,k})$ is an open and dense submanifold of the nonsingular part of $\mathbf{S}\Sigma_m^k$.

We embed $\mathbf{SO}(m) \times \mathbf{SO}(k - 1 - m)$ in $\mathbf{SO}(k - 1)$ by mapping (W_1, W_2) to $W_1 \oplus W_2 = \begin{pmatrix} W_1 & 0 \\ 0 & W_2 \end{pmatrix}$, and we denote by $[V]$ the projection of $V \in \mathbf{SO}(k - 1)$ in the Stiefel manifold

$$\mathbb{V}_{k-1,m} = \frac{\mathbf{SO}(k - 1)}{\{I_m\} \times \mathbf{SO}(k - 1 - m)}$$

of orthonormal m -frames in \mathbb{R}^{k-1} . If we think of \mathbb{R}^{k-1} as the space of row vectors, the frame $[V]$ consists of the first m rows of V —these being left unchanged by $\{I_m\} \times \mathbf{SO}(k - 1 - m)$ acting on the left. We shall also use $[V]$ to denote the corresponding $m \times (k - 1)$ submatrix of V .

We next write Δ for the (maximal abelian) subgroup of diagonal rotations in $\mathbf{SO}(m)$. That is, the elements of Δ are the matrices of the form $D = \text{diag}(\delta_1, \dots, \delta_m)$ with each $\delta_i = \pm 1$ and $\det(D) = 1$, so that the number of minus signs is even. Now Δ acts freely and properly discontinuously on $\mathbb{V}_{k-1,m}$ from the left, so that the quotient map from $\mathbb{V}_{k-1,m}$ to $\mathbb{V}_{k-1,m}/\Delta$ is a normal covering. Hence for any $[V] \in \mathbb{V}_{k-1,m}$ there is an open set in $\mathbb{V}_{k-1,m}$ containing $[V]$ on which the restriction of this quotient map is injective. We denote any such set by $\mathbb{F}_{[V]}$. We now have the following:

LEMMA. For any $\tilde{X}_0 \in \mathbb{X}_{m,k}$ with a singular-values decomposition $\tilde{X}_0 = U_0(\tilde{\Lambda}_0 \ 0)V_0$, the map $\hat{h}_{[V_0]}$ from $\mathbf{SO}(m) \times \mathbb{E}^m \times \mathbb{F}_{[V_0]}$ to $\mathbb{X}_{m,k}$ defined by

$$(U, (x_1, \dots, x_m), [V]) \mapsto U(\text{diag}(x_1, \dots, x_m) \ 0)V$$

is a diffeomorphism onto an open subset of $\mathbb{X}_{m,k}$ containing \tilde{X}_0 . It induces a diffeomorphism of $\mathbb{E}^m \times \mathbb{F}_{[V_0]}$ onto an open neighbourhood of $\pi(\tilde{X}_0)$.

PROOF. Since $(\tilde{\Lambda} \ 0)(I \oplus W)V = (\tilde{\Lambda} \ 0)V$ for any W in $\mathbf{SO}(k - 1 - m)$, it follows that $\hat{h}_{[V_0]}$ is well defined. It is clearly continuous, and its image is open and contains \tilde{X}_0 .

For $\tilde{X} \in \mathbb{X}_{m,k}$, U will be determined up to a right diagonal factor $D \in \Delta$ and the first m rows of V will be determined up to a left diagonal factor

$D' \in \Delta$. That is, \tilde{X} determines the right coset $U\Delta$ of U and the left coset $(\Delta \times \mathbf{SO}(k-1-m))V$ of V . Hence, if $U(\tilde{\Lambda} \ 0)V = U'(\tilde{\Lambda} \ 0)V' = \tilde{X} \in \mathbb{X}_{m,k}$ with $[V], [V'] \in \mathbb{F}_{[V_0]}$ then $U' = UD$ and $(D \oplus I_{k-1-m})V' = (I \oplus W)V$ for some W in $\mathbf{SO}(k-1-m)$, so that $D = I$, $U' = U$ and $[V] = [V']$. This implies that $\hat{h}_{[V_0]}$ is injective. It now suffices, by the inverse function theorem, to show that *the derivative $d\hat{h}_{[V_0]}$ is an isomorphism at each point of the domain.*

To do this, we begin by considering the map H from $\mathbf{SO}(m) \times \mathbb{E}^m \times \mathbf{SO}(k-1)$ to $\mathbb{X}_{m,k}$ defined by

$$(U, (x_1, \dots, x_m), V) \mapsto \tilde{X} = U(\text{diag}(x_1, \dots, x_m) \ 0)V.$$

This map H is differentiable, and locally $H = \hat{h}_{[V_0]} \circ (1 \times 1 \times \pi_0)$, where π_0 denotes the projection $V \mapsto [V]$ of $\mathbf{SO}(k-1)$ on $\mathbb{V}_{k-1,m}$.

To proceed further we need to turn to the study of the differential forms and associated vector fields that will in any case play a leading role in the later metric and curvature calculations.

We define the matrices $\Psi = (\psi_{i,j})$ and $\Phi = (\phi_{i,j})$ of one-forms given by

$$\Psi_U = dU^t U \quad \text{and} \quad \Phi_V = dV V^t$$

which are both skew-symmetric, where $U = (u_{i,j}) \in \mathbf{SO}(m)$, $V = (v_{i,j}) \in \mathbf{SO}(k-1)$ and d denotes the exterior derivative. Here Ψ is left invariant relative to $\mathbf{SO}(m)$, and Φ is right invariant relative to $\mathbf{SO}(k-1)$. The elements of Ψ_U above the diagonal form a basis of $\mathcal{T}_U^*(\mathbf{SO}(m))$ and those in Φ_V form a basis of $\mathcal{T}_V^*(\mathbf{SO}(k-1))$. Thus, in particular, the dual vector fields $\{\xi_{i,j} = \sum_{s=1}^{k-1} v_{js} \partial / \partial v_{is} | 1 \leq i < j \leq k-1\}$ of $\{\phi_{i,j} | 1 \leq i < j \leq k-1\}$ are independent and right invariant relative to $\mathbf{SO}(k-1)$.

The subspace of $\mathcal{T}_V(\mathbf{SO}(k-1))$ along the fibre $\mathcal{P} = \pi_0^{-1}(\pi_0(V)) = (\{I_m\} \times \mathbf{SO}(k-1-m))V$ is the set of $(k-1) \times (k-1)$ matrices $\{(0_m \oplus A) | A^t = -A\}$ with respect to the basis $\{\partial / \partial v_{i,j} | 1 \leq i, j \leq k-1\}$, or equivalently, it is the set of $(k-1) \times (k-1)$ matrices $\{0_m \oplus A | A^t = -A\}$ with respect to the basis $\{\xi_{i,j} | 1 \leq i, j \leq k-1\}$. If we write the matrix Φ_V as

$$\begin{pmatrix} \Phi_1(V) & \Phi_2(V) \\ -\Phi_2(V)^t & \Phi_3(V) \end{pmatrix},$$

then the elements of $\Phi_2(V)$ together with those above the diagonal in $\Phi_1(V)$ will form a basis of $\text{Im}(\pi_0^*)$, which is the same as the annihilator $\mathcal{T}_V(\mathcal{P})^\circ$ of $\mathcal{T}_V(\mathcal{P})$ in $\mathcal{T}_V^*(\mathbf{SO}(k-1))$, while the subspace of $\mathcal{T}_V^*(\mathbf{SO}(k-1))$ spanned by the elements above the diagonal in $\Phi_3(U)$ is a direct complement of $\text{Im}(\pi_0^*)$.

Now the linear map H^* that is the dual of the derivative dH maps the form $U^t d\tilde{X} V^t$ to $-\Psi\tilde{\Lambda} + d\tilde{\Lambda} + \tilde{\Lambda}[\Phi]$. This shows that

$$\text{Im}(H^*) \subset \mathcal{T}_U^*(\mathbf{SO}(m)) \oplus \mathcal{T}_{(x_1, \dots, x_m)}^*(\mathbb{E}^m) \oplus \mathcal{T}_V(\mathcal{P})^\circ,$$

and, after some calculation, we find that H^* maps the $(m \times (k - 1))$ -form $\prod_{i=1}^m \prod_{j=1}^{k-1} dx_{ij}$ to

$$\left\{ \prod_{1 \leq i < j \leq m} (\tilde{\lambda}_j^2 - \tilde{\lambda}_i^2) \prod_{1 \leq i \leq m} \tilde{\lambda}_i^{k-1-m} \right\} \prod_{1 \leq i < j \leq m} \psi_{ij} \prod_{1 \leq i \leq m} d\tilde{\lambda}_i \prod_{\substack{1 \leq i \leq m \\ i < j \leq k-1}} \phi_{ij}.$$

Also

$$\prod_{1 \leq i < j \leq m} (\tilde{\lambda}_j^2 - \tilde{\lambda}_i^2) \prod_{1 \leq i \leq m} \tilde{\lambda}_i^{k-1-m} \neq 0$$

for \tilde{X} in $\mathbb{X}_{m,k}$, so we get $\text{rank}(H^*) = \dim(\mathcal{F}_{\tilde{X}}^*(\mathbb{X}_{m,k}))$ and

$$\text{Im}(H^*) = \mathcal{F}_U^*(\mathbf{SO}(m)) \oplus \mathcal{F}_{(x_1, \dots, x_m)}^*(\mathbb{E}^m) \oplus \mathcal{F}_V(\mathcal{P})^\circ = \text{Im}(1 \times 1 \times \pi_0^*).$$

The facts that $H^* = (1 \times 1 \times \pi_0^*) \circ \hat{h}_{[V_0]}^*$ and that H^* is injective imply that $\hat{h}_{[V_0]}^*$ is injective and hence (because its domain and image have the same dimension) an isomorphism. Then so too is $d\hat{h}_{[V_0]}$.

With $\mathbf{SO}(m)$ acting on the left of $\mathbf{SO}(m) \times \mathbb{E}^m \times \mathbb{F}_{[V_0]}$ by composition in the first factor, $\hat{h}_{[V_0]}$ is equivariant, and hence it induces the injection $h_{[V_0]}$ from $\mathbb{E}^m \times \mathbb{F}_{[V_0]}$ to $\pi(\mathbb{X}_{m,k})$ defined by

$$((x_1, \dots, x_m), [V]) \mapsto \pi((\text{diag}(x_1, \dots, x_m) \ 0)V).$$

Because π is a submersion on $\mathbb{X}_{m,k}$, it follows that $h_{[V_0]}$ is a diffeomorphism onto an open neighbourhood of $\pi(\tilde{X}_0)$. This completes the proof of the lemma. \square

REMARK. Similarly, for X_0 in $\mathbb{S}^{m(k-1)-1} \cap \mathbb{X}_{m,k}$, the restriction of $\hat{h}_{[V_0]}$ to $\mathbf{SO}(m) \times (\mathbb{S}^{m-1} \cap \mathbb{E}^m) \times \mathbb{F}_{[V_0]}$ is a diffeomorphism onto an open subset of $\mathbb{S}^{m(k-1)-1} \cap \mathbb{X}_{m,k}$ containing X_0 , and the restriction of $h_{[V_0]}$ to $(\mathbb{S}^{m-1} \cap \mathbb{E}^m) \times \mathbb{F}_{[V_0]}$ is a diffeomorphism onto an open subset of $\Sigma_m^k \cap \pi(\mathbb{X}_{m,k})$.

REMARK (The continuity principle). The lemma implies that any point $\pi(\tilde{X})$ of $\pi(\mathbb{X}_{m,k})$ can be represented by $(\tilde{\Lambda}, [V])$. Such coordinates can behave disastrously at the points in the complement of $\pi(\mathbb{X}_{m,k})$ where two or more of the absolute values of the $\tilde{\lambda}_i$'s coincide. But if a function on the size-and-shape space that interests us is continuous, then this difficulty can be overcome by taking limits of its values along sequences of points in $\pi(\mathbb{X}_{m,k})$ to evaluate the function on the complement of $\pi(\mathbb{X}_{m,k})$. *This continuity principle will enable us to use $(\tilde{\Lambda}, [V])$ as coordinates whenever there is no need to insist on a global coordinate system.*

In passing we remark that if the points $x_1^*, x_2^*, \dots, x_k^*$ diffuse as independent standard Brownian motions in \mathbb{R}^m , where $m \geq 2$ and $k \geq m + 1$, it has been shown by Bru [6] and by W. S. Kendall [40, 41] that the singular values $\tilde{\lambda}_j$ will almost surely remain noncoincident for all $t > 0$ if they start non-coincident. In particular this implies that with probability 1 the process induced on

$\mathbf{S}\Sigma_m^k$ will stay in $\pi(\mathbb{X}_{m,k})$ and will forever avoid the singularity set, if it starts in $\pi(X_{m,k})$.

5. The Riemannian metrics of $\mathbf{S}\Sigma_m^k$ and Σ_m^k . We are now ready to derive explicit formulae for the Riemannian metric on every size-and-shape space and shape space. The forms of the main results [at (1) and (4) below] owe their elegance to a prudent choice of basic covector and vector fields naturally related to the submersive structure and its Riemannian character. We use these to obtain, as corollaries, (i) the Riemannian volume elements (that will serve as reference measures in the construction of probability densities and distributions of shape statistics), and (ii) the generator of the diffusion on the shape space induced by the Brownian motion on the preshape sphere. Finally in this section we establish a structurally important spectral “nesting principle” that relates each Σ_m^k , $m \leq k - 2$, to a metric subspace of Σ_{k-1}^k .

The linear map π_0^* of the last section is an isomorphism from $\mathcal{T}_{[V]}^*(\mathbb{V}_{k-1,m})$ to $\mathcal{T}_{V'}(\mathcal{P})^\circ$ for any V' in \mathcal{P} , and $\mathcal{T}_{V'}(\mathcal{P})^\circ$ is spanned by the elements of $\Phi_2(V')$ together with those above the diagonal in $\Phi_1(V')$, so $d\pi_0$ is an isomorphism from the subspace of $\mathcal{T}_{V'}(\mathbf{SO}(k-1))$ spanned by $\{\xi_{ij}(V') | 1 \leq i \leq m, i < j \leq k-1\}$ to $\mathcal{T}_{[V]}(\mathbb{V}_{k-1,m})$. In the following we therefore choose any such $V' \in \mathcal{P}$ and denote $d\pi_0(\xi_{ij}(V'))$ in $\mathcal{T}_{[V]}(\mathbb{V}_{k-1,m})$ by $\xi_{ij}([V])$ and similarly denote $\{\pi_0^*\}^{-1}(\phi_{ij}(V'))$ in $\mathcal{T}_{[V]}^*(\mathbb{V}_{k-1,m})$ by $\phi_{ij}([V])$. Then $\{\xi_{ij}([V]) | 1 \leq i \leq m, i < j \leq k-1\}$ is a basis of $\mathcal{T}_{[V]}(\mathbb{V}_{k-1,m})$ and $\{\phi_{ij}([V]) | 1 \leq i \leq m, i < j \leq k-1\}$ is a basis of $\mathcal{T}_{[V]}^*(\mathbb{V}_{k-1,m})$.

More generally, through any V' we can choose a *slice* with respect to the action of $\mathbf{SO}(m)$, that is, a submanifold containing V' which meets each fibre through a neighbourhood of V' once and only once. Such a slice, together with the fields ξ_{ij} and ϕ_{ij} on $\mathbf{SO}(k-1)$, determines vector and covector fields on $\mathbb{V}_{k-1,m}$ that we also denote by ξ_{ij} and ϕ_{ij} , respectively.

Note that Φ_1 is left invariant relative to $\mathbf{SO}(k-1-m)$, or equivalently, for any W in $\mathbf{SO}(k-1-m)$, $L_W^* \Phi_1((I \oplus W)V) = \Phi_1(V)$. Thus $\{\phi_{ij}([V]) | 1 \leq i < j \leq m\}$ and $\{\xi_{ij}([V]) | 1 \leq i < j \leq m\}$ are independent of the choice of V' used to define them. The same cannot be said for $\Phi_2([V])$ and $\{\xi_{ij}([V]) | 1 \leq i \leq m < j \leq k-1\}$ since $L_W^* \Phi_2((I \oplus W)V) = \Phi_2(V)W^t$. However the $[\Phi][\Phi]^t$ is invariant and the corresponding two-forms on $\mathbb{V}_{k-1,m}$, required below to express the metrics of $\mathbf{S}\Sigma_m^k$ and Σ_m^k , are well defined. We now have the following result for the size-and-shape space.

THEOREM 1. *The Riemannian metric of $\mathbf{S}\Sigma_m^k$, restricted to $\pi(\mathbb{X}_{m,k})$, is*

$$(1) \quad \sum_{i=1}^m d\tilde{\lambda}_i^2 + \sum_{1 \leq i < j \leq m} \frac{(\tilde{\lambda}_i^2 - \tilde{\lambda}_j^2)^2}{\tilde{\lambda}_i^2 + \tilde{\lambda}_j^2} \phi_{ij}^2 + \sum_{i=1}^m \sum_{j=m+1}^{k-1} \tilde{\lambda}_i^2 \phi_{ij}^2.$$

Note that the quadratic form in the theorem is purely diagonal, and that when $k = m + 1$ then the last term in the formula for the metric disappears.

PROOF. $\mathbb{X}_{m,k}$ is locally a product manifold $\mathbf{SO}(m) \times \mathbb{E}^m \times \mathbb{F}_{[V_0]}$, and so for \tilde{X} in $\mathbb{X}_{m,k}$, $\mathcal{F}_{\tilde{X}}(\mathbb{R}^{m(k-1)})$ is isomorphic with $\mathcal{F}_U(\mathbf{SO}(m)) \oplus \mathcal{F}_{(\tilde{\lambda}_1, \dots, \tilde{\lambda}_m)}(\mathbb{E}^m) \oplus \mathcal{F}_{[V]}(\mathbb{V}_{k-1, m})$. The Riemannian metric of the flat space $\mathbb{R}^{m(k-1)}$ is given by $\text{tr}(d\tilde{X}^t d\tilde{X})$. In terms of the basis

$$\{\psi_{ij} | 1 \leq i < j \leq m\} \cup \{d\tilde{\lambda}_i | 1 \leq i \leq m\} \cup \{\phi_{ij} | 1 \leq i \leq m, i < j \leq k-1\}$$

of the direct sum

$$\mathcal{F}_U^*(\mathbf{SO}(m)) \oplus \mathcal{F}_{(\tilde{\lambda}_1, \dots, \tilde{\lambda}_m)}^*(\mathbb{E}^m) \oplus \mathcal{F}_{[V]}^*(\mathbb{V}_{k-1, m}),$$

the metric $\text{tr}(d\tilde{X}^t d\tilde{X})$ can be expressed as

the trace of $\left\{ (d\tilde{\Lambda})^2 + \tilde{\Lambda}^2[\Phi][\Phi]^t + 2\tilde{\Lambda}\Psi\tilde{\Lambda}\Phi_1 - \tilde{\Lambda}^2\Psi^2 \right\}$

$$(2) \quad = \sum_{i=1}^m d\tilde{\lambda}_i^2 + \sum_{1 \leq i < j \leq m} \frac{(\tilde{\lambda}_i^2 - \tilde{\lambda}_j^2)^2}{\tilde{\lambda}_i^2 + \tilde{\lambda}_j^2} \phi_{ij}^2 + \sum_{i=1}^m \sum_{j=m+1}^{k-1} \tilde{\lambda}_i^2 \phi_{ij}^2$$

$$+ \sum_{1 \leq i < j \leq m} (\tilde{\lambda}_i^2 + \tilde{\lambda}_j^2) \left(\psi_{ij} - 2 \frac{\tilde{\lambda}_i \tilde{\lambda}_j}{\tilde{\lambda}_i^2 + \tilde{\lambda}_j^2} \phi_{ij} \right)^2.$$

Let us denote by η_{ij} the dual vector fields of ψ_{ij} . Then $\{\eta_{ij} | 1 \leq i < j \leq m\}$, clearly independent and left invariant relative to $\mathbf{SO}(m)$, are by definition tangent to the fibres of the submersion. All the other vector fields $\{\partial/\partial\tilde{\lambda}_i | 1 \leq i \leq m\} \cup \{\xi_{ij} | 1 \leq i \leq m, i < j \leq k-1\}$ that we have used are transverse to such “vertical” vectors. Indeed formula (2) makes it clear that (i) the vector fields $\{\partial/\partial\tilde{\lambda}_i | 1 \leq i \leq m\}$ and $\{\xi_{ij} | 1 \leq i \leq m < j \leq k-1\}$ are actually orthogonal to the fibres and so are “horizontal” vector fields, that (ii) the horizontal versions of $\{\xi_{ij} | 1 \leq i < j \leq m\}$ are

$$\bar{\xi}_{ij} = \xi_{ij} + 2 \frac{\tilde{\lambda}_i \tilde{\lambda}_j}{\tilde{\lambda}_i^2 + \tilde{\lambda}_j^2} \eta_{ij}, \quad 1 \leq i < j \leq m,$$

and that (iii)

$$\langle \bar{\xi}_{ij}, \bar{\xi}_{i'j'} \rangle = \frac{(\tilde{\lambda}_i^2 - \tilde{\lambda}_j^2)^2}{\tilde{\lambda}_i^2 + \tilde{\lambda}_j^2} \delta_{i'i'} \delta_{j'j'}.$$

Now it follows from O’Neill [54] that the collection of horizontal vector fields on $\mathbb{R}^{m(k-1)}$ will map bijectively under the submersion onto the complete collection of vector fields on $X_{m,k}$ in the size-and-shape space, and that the Riemannian scalar product of any two horizontal vector fields at such a point of $\mathbb{R}^{m(k-1)}$ will be equal to the Riemannian scalar product of the image fields at the image point of $\mathbf{S}\Sigma_m^k$. The proof of the theorem is therefore complete. \square

In order to be able to formulate a similar result for the shape spaces we write $\lambda_i = \tilde{\lambda}_i/r$. Then $\sum \lambda_i^2 = 1$. Using for convenience the customary stereographic coordinates u_1, u_2, \dots, u_{m-1} on this sphere, given by the formula

$$(3) \quad u_i = \frac{\lambda_{i+1}}{1 + \lambda_1}, \quad 1 \leq i \leq m - 1,$$

we get the following:

THEOREM 2. *The Riemannian metric of Σ_m^k , restricted to $\Sigma_m^k \cap \pi(\mathbb{X}_{m,k})$, is*

$$(4) \quad (1 + \lambda_1)^2 \sum_{i=1}^{m-1} du_i^2 + \sum_{1 \leq i < j \leq m} \frac{(\lambda_i^2 - \lambda_j^2)^2}{\lambda_i^2 + \lambda_j^2} \phi_{ij}^2 + \sum_{i=1}^m \sum_{j=m+1}^{k-1} \lambda_i^2 \phi_{ij}^2.$$

Here again the quadratic form is purely diagonal, and the double-summation term disappears when $k = m + 1$.

PROOF. $\mathbf{S}\Sigma_m^k$ is a warped product of the half line \mathbb{R}_+ for size r and Σ_m^k with the warping function r^2 , so that the warped metric ρ of $\mathbf{S}\Sigma_m^k \setminus \pi(\mathcal{S}_{m,k})$ is given (cf. O'Neill [56]) by

$$d\rho^2 = dr^2 + r^2 ds^2,$$

where ds^2 represents the Riemannian metric of $\Sigma_m^k \setminus \pi(\mathcal{S}_{m,k})$. It is easy to check that

$$\sum_{i=1}^m d\tilde{\lambda}_i^2 = dr^2 + r^2 \left\{ \sum_{i=2}^m \left(d \frac{\tilde{\lambda}_i}{r} \right)^2 + \left(\sum_{i=2}^m \frac{\tilde{\lambda}_i}{\tilde{\lambda}_1} d \frac{\tilde{\lambda}_i}{r} \right)^2 \right\},$$

and hence (1) can be rewritten as

$$dr^2 + r^2 \left\{ \sum_{i=2}^m d\lambda_i^2 + \left(\sum_{i=2}^m \frac{\lambda_i}{\lambda_1} d\lambda_i \right)^2 + \sum_{1 \leq i < j \leq m} \frac{(\lambda_i^2 - \lambda_j^2)^2}{\lambda_i^2 + \lambda_j^2} \phi_{ij}^2 + \sum_{i=1}^m \sum_{j=m+1}^{k-1} \lambda_i^2 \phi_{ij}^2 \right\}.$$

Thus

$$(5) \quad ds^2 = \sum_{i=2}^m d\lambda_i^2 + \left(\sum_{i=2}^m \frac{\lambda_i}{\lambda_1} d\lambda_i \right)^2 + \sum_{1 \leq i < j \leq m} \frac{(\lambda_i^2 - \lambda_j^2)^2}{\lambda_i^2 + \lambda_j^2} \phi_{ij}^2 + \sum_{i=1}^m \sum_{j=m+1}^{k-1} \lambda_i^2 \phi_{ij}^2.$$

The theorem immediately follows from formula (3). \square

REMARK. The vectors $\partial/\partial\lambda_2, \dots, \partial/\partial\lambda_m$, supplemented by $\{\xi_{ij} | 1 \leq i \leq m, i < j \leq k-1\}$, also form a basis of $\mathcal{T}_{\pi(X)}(\Sigma_m^k)$ for $\pi(X)$ in $\Sigma_m^k \cap \pi(\mathbb{X}_{m,k})$. Formula (5) gives an equivalent expression for the Riemannian metric on $\Sigma_m^k \cap \pi(\mathbb{X}_{m,k})$ in terms of this basis, which will no longer be diagonal. However the coordinates $\lambda_2, \dots, \lambda_m$ here have a simpler relation with the coordinates $\tilde{\lambda}_1, \dots, \tilde{\lambda}_m$ that we used in the size-and-shape space. We shall use this basis from time to time, and in particular we shall use formula (5) to obtain the Ricci curvature tensor of the shape spaces.

COROLLARY 1. *The volume element of $\mathbf{S}\Sigma_m^k$ is*

$$\prod_{i=1}^m |\tilde{\lambda}_i|^{k-1-m} \prod_{1 \leq i < j \leq m} \frac{|\tilde{\lambda}_i^2 - \tilde{\lambda}_j^2|}{\sqrt{\tilde{\lambda}_i^2 + \tilde{\lambda}_j^2}} \prod_{i=1}^m d\tilde{\lambda}_i \prod_{i=1}^m \prod_{j=i+1}^{k-1} \phi_{ij},$$

and the volume element of Σ_m^k is

$$(1 + \lambda_1)^{m-1} \prod_{i=1}^m |\lambda_i|^{k-1-m} \prod_{1 \leq i < j \leq m} \frac{|\lambda_i^2 - \lambda_j^2|}{\sqrt{\lambda_i^2 + \lambda_j^2}} \prod_{i=1}^{m-1} du_i \prod_{i=1}^m \prod_{j=i+1}^{k-1} \phi_{ij}.$$

It would be interesting to know the values of the integrals of these two volume elements over the size-and-shape space and the shape-space, respectively, because one could then norm them to become probability elements.

Note that $\prod_{i=1}^m \prod_{j=i+1}^{k-1} \phi_{ij}$ is independent of the choice of V' . Note also that $\prod_{i=1}^m \prod_{j=i+1}^{k-1} \phi_{ij}$ is invariant relative to the transformations $[V] \mapsto W[V]$ for W in $\mathbf{SO}(m)$ and $[V] \mapsto [V]W$ for W in $\mathbf{SO}(k-1)$. Hence $\prod_{i=1}^m \prod_{j=i+1}^{k-1} \phi_{ij}$ defines a constant multiple of the usual invariant measure on $\mathbb{V}_{k-1,m}$.

COROLLARY 2. *The volume of the fibre $\pi^{-1}(\pi(\tilde{X}))$ above any nonsingular point $\pi(\tilde{X})$ is*

$$\gamma_{k,m} \prod_{1 \leq i < j \leq m} \sqrt{\tilde{\lambda}_i^2 + \tilde{\lambda}_j^2}$$

for some positive constant $\gamma_{k,m}$.

Note that this coincides with the expression found by Carne [7], where however the square root was overlooked.

PROOF. It follows immediately from (2) that the volume element of the fibre $\pi^{-1}(\pi(\tilde{X}))$ for any $\pi(\tilde{X})$ in $\pi(\mathbb{X}_{m,k})$ is

$$\prod_{1 \leq i < j \leq m} \sqrt{\tilde{\lambda}_i^2 + \tilde{\lambda}_j^2} \prod_{1 \leq i < j \leq m} \psi_{ij},$$

and so the expression for the volume of the fibre holds for $\pi(\tilde{X})$ in $\pi(\mathbb{X}_{m,k})$. Then by the continuity principle it is also true for any nonsingular point. \square

COROLLARY 3. *Brownian motion on $\mathbb{S}^{m(k-1)-1}$ induces a shape diffusion on Σ_m^k that is a Brownian motion with drift*

$$(6) \quad \sum_{i=2}^m \left\{ \sum_{j \neq i} \frac{\lambda_i}{\lambda_i^2 + \lambda_j^2} - \frac{1}{2} m(m-1) \lambda_i \right\} \frac{\partial}{\partial \lambda_i}.$$

PROOF. For $\pi(X)$ in $\Sigma_m^k \setminus \pi(\mathcal{S}_{m,k})$, the field (6) is $\text{grad}\{\log(\text{volume of } \pi^{-1}(\pi(X)))\}$. \square

Note that $k - 1$ labelled independent Brownian motions on \mathbb{R}^m induce a Brownian motion on $\mathbb{S}^{m(k-1)-1}$ with respect to the random time τ defined by $d\tau = dt/r^2$ (Rogers and Williams [58]). Thus we have from the above corollary that k labelled independent Brownian motions on \mathbb{R}^m induce a shape diffusion on Σ_m^k which, with respect to the random time τ , is a Brownian motion with drift as at (6) above, because the map used to remove the centroid of the data matrix X^* is orthogonal. \square

REMARK (The nesting principle). The Riemannian metric of the shape space Σ_{k-1}^k restricted to $\Sigma_{k-1}^k \cap \pi(\mathbb{X}_{k-1,k})$ is

$$(1 + \lambda_1)^2 \sum_{i=1}^{k-2} du_i^2 + \sum_{1 \leq i < j \leq k-1} \frac{(\lambda_i^2 - \lambda_j^2)^2}{\lambda_i^2 + \lambda_j^2} \phi_{ij}^2.$$

If $k - 1 > m$ and if in this formula we write $\lambda_i = 0$ for $i > m$ (whence also $u_i = 0$ for $i \geq m$), we obtain *exactly* the Riemannian metric on $\Sigma_m^k \cap \pi(\mathbb{X}_{m,k})$. This is what we shall call *the nesting principle*.

The “explanation” of this important result is as follows. The $(k - 1) \times (k - 1)$ matrices of $\mathbb{S}^{(k-1)^2-1}$ of rank m or less are characterized by $\lambda_i = 0$ for $i > m$ and can be arranged, using the left action of $\mathbf{SO}(k - 1)$, to have their last $k - 1 - m$ rows zero. In this way such preshapes can be identified with the preshapes of Σ_m^k supplemented by the appropriate number of zero rows. Now the shape space Σ_m^k consists of two parts which are mapped isometrically onto each other under left multiplication by the matrix $D = \text{diag}(1, \dots, 1, -1)$. However, once embedded as above in $\mathbb{S}^{(k-1)^2-1}$ with $k - 1 - m \geq 1$ zero rows adjoined, the preshapes X and DX determine the same shape in Σ_{k-1}^k . Thus *nested inside Σ_{k-1}^k we have an isometric copy of Σ_m^k/\mathbb{Z}_2 . More generally, for any $r < s \leq k - 1$, Σ_s^k contains an isometric copy of Σ_r^k/\mathbb{Z}_2 . In particular, the singularity set $\pi(\mathcal{S}_{m,k}) \cap \Sigma_m^k$ of Σ_m^k is isometric with $\Sigma_{m-2}^k/\mathbb{Z}_2$ and hence, since this has a lower dimension, it is of measure zero. A similar nesting principle holds for the size-and-shape spaces with similar consequences.*

A useful observation is that (3) can be replaced by

$$u_i = \frac{\lambda_i}{1 + \lambda_r}, \quad i < r \quad \text{and} \quad u_i = \frac{\lambda_{i+1}}{1 + \lambda_r}, \quad r \leq i \leq m - 1$$

when convenient. Then (3) is the case $r = 1$, and in the general case the metric will still be given by Theorem 2 except that the term $(1 + \lambda_1)^2$ will be replaced by $(1 + \lambda_r)^2$.

6. The curvature of the size-and-shape space $S\Sigma_m^k$. We now turn to the calculation of curvatures. A guiding principle here is the famous theorem of O'Neill showing how, when passing from the "top" space to the "bottom" space of a Riemannian submersion, *the sectional curvatures never decrease*. This is the reason why the sectional curvatures for the size-and-shape space in Theorem 3 are always nonnegative, because the presize-and-shape space is flat (has zero curvature).

As another notable consequence of the O'Neill theory in this application we shall find that some of the nonzero sectional curvatures of the size-and-shape space tend to positive infinity as one approaches a singularity.

Recall that, on $\mathbb{X}_{m,k}$, the η_{ij} 's constitute a basis for the vertical vector fields, while the $\partial/\partial\tilde{\lambda}_i$'s, ξ_{ij} 's and $\bar{\xi}_{ij}$'s for the appropriate pairs (i, j) constitute a basis for the horizontal vector fields, the verticality and horizontality being with respect to the Riemannian submersion π . Also each pair of fields drawn from the combined (horizontal and vertical) basis is orthogonal with respect to the metric but may not be orthonormal.

The basic measure of curvature is the Riemannian curvature tensor. We now apply O'Neill's theorem [54] on the curvature of submersions, which in this case (because the curvature of $\mathbb{R}^{m(k-1)}$ is identically zero) says that *if, for each i , $\bar{\zeta}_i$ is the horizontal lift to $\mathbb{R}^{m(k-1)}$ of the vector ζ_i tangent to $S\Sigma_m^k \setminus \pi(\mathcal{L}_{m,k})$, then the Riemannian curvature tensor $R_{S\Sigma_m^k}$ of $S\Sigma_m^k \setminus \pi(\mathcal{L}_{m,k})$ is given by*

$$(7) \quad \begin{aligned} \langle R_{S\Sigma_m^k}(\zeta_1, \zeta_2)\zeta_3, \zeta_4 \rangle &= \frac{1}{2} \langle [\bar{\zeta}_1, \bar{\zeta}_2]^v, [\bar{\zeta}_3, \bar{\zeta}_4]^v \rangle \\ &\quad - \frac{1}{4} \langle [\bar{\zeta}_2, \bar{\zeta}_3]^v, [\bar{\zeta}_1, \bar{\zeta}_4]^v \rangle - \frac{1}{4} \langle [\bar{\zeta}_3, \bar{\zeta}_1]^v, [\bar{\zeta}_2, \bar{\zeta}_4]^v \rangle, \end{aligned}$$

where the $[\dots]^v$ indicates that it is the "vertical part" that is required.

The only pairs of horizontal vector fields from our chosen basis whose Lie brackets can contribute anything to the Riemannian curvature are among those of the forms $(\partial/\partial\tilde{\lambda}_r, \bar{\xi}_{ij})$ and $(\bar{\xi}_{i_1 j_1}, \bar{\xi}_{i_2 j_2})$. Their Lie brackets are

$$(8) \quad \begin{aligned} \left[\frac{\partial}{\partial\tilde{\lambda}_r}, \bar{\xi}_{ij} \right] &= 2 \frac{\partial}{\partial\tilde{\lambda}_r} \left\{ \frac{\tilde{\lambda}_i \tilde{\lambda}_j}{\tilde{\lambda}_i^2 + \tilde{\lambda}_j^2} \right\} \eta_{ij}, \\ [\bar{\xi}_{i_1 j_1}, \bar{\xi}_{i_2 j_2}] &= [\xi_{i_1 j_1}, \xi_{i_2 j_2}] + 4 \frac{\tilde{\lambda}_{i_1} \tilde{\lambda}_{j_1}}{\tilde{\lambda}_{i_1}^2 + \tilde{\lambda}_{j_1}^2} \frac{\tilde{\lambda}_{i_2} \tilde{\lambda}_{j_2}}{\tilde{\lambda}_{i_2}^2 + \tilde{\lambda}_{j_2}^2} [\eta_{i_1 j_1}, \eta_{i_2 j_2}], \end{aligned}$$

respectively, where

$$\begin{aligned} [\eta_{i_1 j_1}, \eta_{i_2 j_2}] &= \delta_{i_1 j_2} \eta_{i_2 j_1} + \delta_{i_2 j_1} \eta_{j_2 i_1} + \delta_{i_1 i_2} \eta_{j_1 j_2} + \delta_{j_1 j_2} \eta_{i_1 i_2}, \\ [\xi_{i_1 j_1}, \xi_{i_2 j_2}] &= \delta_{i_1 j_2} \xi_{i_2 j_1} + \delta_{i_2 j_1} \xi_{j_2 i_1} + \delta_{i_1 i_2} \xi_{j_1 j_2} + \delta_{j_1 j_2} \xi_{i_1 i_2}. \end{aligned}$$

Hence $[\partial/\partial\bar{\lambda}_r, \bar{\xi}_{ij}]^v \neq 0$ if and only if $r = i$ or j , and $[\bar{\xi}_{i_1 j_1}, \bar{\xi}_{i_2 j_2}]^v \neq 0$ if and only if $\{i_1, j_1\} \cap \{i_2, j_2\}$ is nonempty. Note that here we have identified $\eta_{ij} = -\eta_{ji}$ and $\xi_{ij} = -\xi_{ji}$. Using these symmetries, and those of the Lie bracket, the following gives all the nonzero terms required for (7):

$$\begin{aligned} (9) \quad \left[\frac{\partial}{\partial\bar{\lambda}_i}, \bar{\xi}_{ij} \right]^v &= 2\bar{\lambda}_j \frac{\bar{\lambda}_j^2 - \bar{\lambda}_i^2}{(\bar{\lambda}_i^2 + \bar{\lambda}_j^2)^2} \eta_{ij}, \\ [\bar{\xi}_{ij}, \bar{\xi}_{i'j'}]^v &= \left\{ 4 \frac{\bar{\lambda}_i \bar{\lambda}_j}{\bar{\lambda}_i^2 + \bar{\lambda}_j^2} \frac{\bar{\lambda}_i \bar{\lambda}_{j'}}{\bar{\lambda}_i^2 + \bar{\lambda}_{j'}^2} - 2 \frac{\bar{\lambda}_j \bar{\lambda}_{j'}}{\bar{\lambda}_j^2 + \bar{\lambda}_{j'}^2} \right\} \eta_{jj'}. \end{aligned}$$

Formulae (7) and (9) allow us to compute the Riemannian curvature on $\pi(X_{m,k})$. In order to compute the Ricci and sectional curvatures there it suffices to evaluate the terms with $\zeta_2 = \zeta_4$. In this case, (7) reduces to

$$(10) \quad \langle R_{\mathbf{S}\Sigma_m^k}(\zeta_1, \zeta)\zeta_2, \zeta \rangle = \frac{3}{4} \langle [\bar{\zeta}, \bar{\zeta}_1]^v, [\bar{\zeta}, \bar{\zeta}_2]^v \rangle.$$

Then a straightforward calculation using (9) shows that, up to the symmetries of the Riemannian curvature tensor, the only nonzero components of the above form are the following:

$$\begin{aligned} \langle R(\xi_{ij}, \xi_{rs})\xi_{ij}, \xi_{rs} \rangle &= \langle R(\xi_{ij}, \xi_{sr})\xi_{ij}, \xi_{sr} \rangle \\ &= 3\bar{\lambda}_s^2 (\bar{\lambda}_i^2 + \bar{\lambda}_j^2 - \bar{\lambda}_r^2) \\ &\quad \times \frac{(\bar{\lambda}_s^2 - \bar{\lambda}_r^2)^2}{\bar{\lambda}_s^2 + \bar{\lambda}_r^2} \frac{(\bar{\lambda}_i^2 - \bar{\lambda}_j^2)^2}{(\bar{\lambda}_i^2 + \bar{\lambda}_j^2)^2 (\bar{\lambda}_i^2 + \bar{\lambda}_s^2)(\bar{\lambda}_j^2 + \bar{\lambda}_s^2)} \end{aligned}$$

if $r = i$ or $j, s \neq i, j$,

$$\begin{aligned} (11) \quad \left\langle R\left(\xi_{ij}, \frac{\partial}{\partial\bar{\lambda}_r}\right)\xi_{ij}, \frac{\partial}{\partial\bar{\lambda}_r}\right\rangle &= 3(\bar{\lambda}_i^2 + \bar{\lambda}_j^2 - \bar{\lambda}_r^2) \frac{(\bar{\lambda}_i^2 - \bar{\lambda}_j^2)^2}{(\bar{\lambda}_i^2 + \bar{\lambda}_j^2)^3} \quad \text{if } r = i \text{ or } j, \\ \left\langle R\left(\frac{\partial}{\partial\bar{\lambda}_i}, \xi_{ij}\right)\frac{\partial}{\partial\bar{\lambda}_j}, \xi_{ij}\right\rangle &= -3\bar{\lambda}_i \bar{\lambda}_j \frac{(\bar{\lambda}_i^2 - \bar{\lambda}_j^2)^2}{(\bar{\lambda}_i^2 + \bar{\lambda}_j^2)^3}, \end{aligned}$$

where $1 \leq i < j \leq m$.

Therefore, we have the following results.

THEOREM 3. *All the sectional curvatures of $\mathbf{S}\Sigma_m^k \setminus \pi(\mathcal{S}_{m,k})$, restricted to $\pi(\times_{m,k})$, associated with the distinct pairs of vectors from the chosen basis are zero save for*

$$K\left(\frac{\partial}{\partial \tilde{\lambda}_r}, \xi_{ij}\right) = 3 \frac{\tilde{\lambda}_i^2 + \tilde{\lambda}_j^2 - \tilde{\lambda}_r^2}{(\tilde{\lambda}_i^2 + \tilde{\lambda}_j^2)^2} \text{ if } r = i \text{ or } j,$$

$$K(\xi_{ij}, \xi_{rs}) = K(\xi_{ij}, \xi_{sr})$$

$$= 3 \frac{\tilde{\lambda}_s^2(\tilde{\lambda}_i^2 + \tilde{\lambda}_j^2 - \tilde{\lambda}_r^2)}{(\tilde{\lambda}_i^2 + \tilde{\lambda}_j^2)(\tilde{\lambda}_i^2 + \tilde{\lambda}_s^2)(\tilde{\lambda}_j^2 + \tilde{\lambda}_s^2)}, \text{ if } r = i \text{ or } j, s \neq i, j.$$

PROOF. By definition the sectional curvature of the tangent plane spanned by the orthogonal vectors ζ_1 and ζ_2 is

$$\langle R_{\mathbf{S}\Sigma_m^k}(\zeta_1, \zeta_2)\zeta_1, \zeta_2 \rangle / (\|\zeta_1\|^2 \|\zeta_2\|^2),$$

which by (10) is $3\|\bar{\zeta}_1, \bar{\zeta}_2\|^2 / (4\|\zeta_1\|^2 \|\zeta_2\|^2)$. The theorem follows from (1), (2) and (11). \square

Notice that $\lambda_{m-1} = \lambda_m = 0$ at a singularity, so that some of the sectional curvatures tend to $+\infty$ there.

Let us denote by $d_{m,k}^s$ the dimension of $\mathbf{S}\Sigma_m^k$, which is equal to $m(2k - m - 1)/2$. Then we have the following:

THEOREM 4. *The $d_{m,k}^s \times d_{m,k}^s$ matrix $M_{m,k}$ of the components of the Ricci curvature tensor Ric of $\mathbf{S}\Sigma_m^k \setminus \pi(\mathcal{S}_{m,k})$, restricted to $\pi(\times_{m,k})$, with respect to the given vector fields has the form*

$$\begin{pmatrix} R_1 & 0 & 0 \\ 0 & R_2 & 0 \\ 0 & 0 & 0 \end{pmatrix},$$

where R_1 is the $m \times m$ matrix, whose (i, j) th entry $\text{Ric}(\partial/\partial \tilde{\lambda}_i, \partial/\partial \tilde{\lambda}_j)$ is

$$-3 \frac{\tilde{\lambda}_i \tilde{\lambda}_j}{(\tilde{\lambda}_i^2 + \tilde{\lambda}_j^2)^2} \text{ if } i \neq j \text{ and } 3 \sum_{s \neq i} \frac{\tilde{\lambda}_s^2}{(\tilde{\lambda}_i^2 + \tilde{\lambda}_s^2)^2} \text{ if } i = j;$$

and R_2 is the $m(m - 1)/2 \times m(m - 1)/2$ diagonal matrix, whose $((i_1, j_1), (i_2, j_2))$ th entry $\text{Ric}(\xi_{i_1 j_1}, \xi_{i_2 j_2})$, $1 \leq i_1 < j_1 \leq m$, $1 \leq i_2 < j_2 \leq m$, is

zero unless $i_1 = i_2 = i$ and $j_1 = j_2 = j$ when it is

$$3 \frac{(\tilde{\lambda}_i^2 - \tilde{\lambda}_j^2)^2}{(\tilde{\lambda}_i^2 + \tilde{\lambda}_j^2)} \sum_{s=1}^m \frac{\tilde{\lambda}_s^2}{(\tilde{\lambda}_i^2 + \tilde{\lambda}_s^2)(\tilde{\lambda}_j^2 + \tilde{\lambda}_s^2)}.$$

Since for any $\mathbf{v} = (v_1, \dots, v_m)$

$$\mathbf{v}R_1\mathbf{v}^t = \frac{3}{2} \sum_{i \neq j} \left\langle \frac{v_i \tilde{\lambda}_j - v_j \tilde{\lambda}_i}{\tilde{\lambda}_i^2 + \tilde{\lambda}_j^2} \right\rangle^2 \geq 0,$$

it follows that the Ricci curvature tensor field Ric on $\pi(\mathbb{X}_{m,k})$ is nonnegative.

PROOF. The Ricci curvature tensor Ric is defined, at each point $\pi(\tilde{X})$ of $\mathbf{S}\Sigma_m^k \setminus \pi(\mathcal{S}_{m,k})$, to be the trace of the endomorphism of $\mathcal{T}_{\pi(\tilde{X})}(\mathbf{S}\Sigma_m^k)$ given by $\zeta \mapsto R_{\mathbf{S}\Sigma_m^k}(\zeta_1, \zeta)\zeta_2$. That is, Ric is the symmetric (0, 2)-tensor given by

$$\text{Ric}(\zeta_1, \zeta_2) = \sum_i \langle R_{\mathbf{S}\Sigma_m^k}(\zeta_1, e_i)\zeta_2, e_i \rangle \|e_i\|^{-2},$$

where the $\{e_i\}$ are $d_{m,k}^s$ orthogonal vector fields on $\mathbf{S}\Sigma_m^k \setminus \pi(\mathcal{S}_{m,k})$. This implies by (11) that the nonzero components of the Ricci curvature tensor on $\pi(\mathbb{X}_{m,k})$ associated with the given vector fields are

$$\begin{aligned} \text{Ric}\left(\frac{\partial}{\partial \tilde{\lambda}_i}, \frac{\partial}{\partial \tilde{\lambda}_j}\right) &= \left\langle R\left(\frac{\partial}{\partial \tilde{\lambda}_i}, \xi_{ij}\right) \frac{\partial}{\partial \tilde{\lambda}_j}, \xi_{ij} \right\rangle \|\xi_{ij}\|^{-2}, \quad i \neq j, \\ \text{Ric}\left(\frac{\partial}{\partial \tilde{\lambda}_i}, \frac{\partial}{\partial \tilde{\lambda}_i}\right) &= \sum_{s \neq i} \left\langle R\left(\frac{\partial}{\partial \tilde{\lambda}_i}, \xi_{is}\right) \frac{\partial}{\partial \tilde{\lambda}_i}, \xi_{is} \right\rangle \|\xi_{is}\|^{-2}, \\ \text{Ric}(\xi_{ij}, \xi_{ij}) &= \left\langle R\left(\xi_{ij}, \frac{\partial}{\partial \tilde{\lambda}_i}\right) \xi_{ij}, \frac{\partial}{\partial \tilde{\lambda}_i} \right\rangle + \left\langle R\left(\xi_{ij}, \frac{\partial}{\partial \tilde{\lambda}_j}\right) \xi_{ij}, \frac{\partial}{\partial \tilde{\lambda}_j} \right\rangle \\ &\quad + \sum_{s \neq i, j} \langle R(\xi_{ij}, \xi_{si})\xi_{ij}, \xi_{si} \rangle \|\xi_{si}\|^{-2} \\ &\quad + \sum_{s \neq i, j} \langle R(\xi_{ij}, \xi_{js})\xi_{ij}, \xi_{js} \rangle \|\xi_{js}\|^{-2}, \quad 1 \leq i < j \leq m, \end{aligned}$$

and so we get the theorem. \square

COROLLARY . The scalar curvature of $\mathbf{S}\Sigma_m^k \setminus \pi(\mathcal{S}_{m,k})$ is

$$(12) \quad 3 \sum_{1 \leq i < j \leq m} \left\{ \frac{1}{\tilde{\lambda}_i^2 + \tilde{\lambda}_j^2} + \sum_{s=1}^m \frac{\tilde{\lambda}_s^2}{(\tilde{\lambda}_i^2 + \tilde{\lambda}_s^2)(\tilde{\lambda}_j^2 + \tilde{\lambda}_s^2)} \right\}.$$

Note that the scalar curvature of $\mathbf{S}\Sigma_m^k \setminus \pi(\mathcal{S}_{m,k})$ is everywhere positive and that it tends to infinity at every one of the singularities.

An important consequence of (12) is that the scalar curvature of $\mathbf{S}\Sigma_m^k \setminus \pi(\mathcal{S}_{m,k})$ will depend only on m for $k > m$. For $k \leq m$, its scalar curvature will depend only on k , because $\mathbf{S}\Sigma_m^k$ is isometric with $\mathbf{S}\Sigma_{k-1}^k/\mathbb{Z}_2$.

PROOF. That the scalar curvature on $\pi(\mathbb{X}_{m,k})$ is given by (12) follows immediately from the fact that the scalar curvature is the metric contraction of the Ricci curvature tensor, or from the fact that the scalar curvature is equal to the sum of the sectional curvatures of tangent two-planes associated with *distinct* pairs of members of an orthogonal basis of tangent vectors. We obtain the corollary by the continuity principle. \square

7. The curvature of the shape space Σ_m^k . Finally we discuss the curvature properties of the shape spaces Σ_m^k themselves. Here the “top” space is a sphere of radius 1, so it will turn out (Theorem 5) that *all* the sectional curvatures of each shape space are greater than or equal to unity, and that some of them tend to positive infinity as one approaches a singularity. Accordingly the scalar curvature tends to infinity as one approaches any of the singularities.

We can investigate the curvature of $\Sigma_m^k \setminus \pi(\mathcal{S}_{m,k})$ in two different ways. We can use either its characterization as the Riemannian quotient space of $\mathbb{S}^{m(k-1)-1}$ (away from the singularities), or the fact that $\mathbf{S}\Sigma_m^k$ is a warped product of \mathbb{R}_+ with Σ_m^k . The advantage of the first method is that, since $\mathbb{S}^{m(k-1)-1}$ has a constant sectional curvature equal to unity, its Riemannian curvature tensor is given by

$$R_{\mathbb{S}^{m(k-1)-1}}(\zeta_1, \zeta_2)\zeta = \langle \zeta, \zeta_1 \rangle \zeta_2 - \langle \zeta, \zeta_2 \rangle \zeta_1.$$

Then, following an argument similar to that in the last section, we shall find that the Riemannian curvature tensor of $\Sigma_m^k \setminus \pi(\mathcal{S}_{m,k})$ is given by

$$\begin{aligned} \langle R_{\Sigma_m^k}(\zeta_1, \zeta_2)\zeta_3, \zeta_4 \rangle &= \langle \bar{\zeta}_3, \bar{\zeta}_1 \rangle \langle \bar{\zeta}_2, \bar{\zeta}_4 \rangle - \langle \bar{\zeta}_3, \bar{\zeta}_2 \rangle \langle \bar{\zeta}_1, \bar{\zeta}_4 \rangle \\ (13) \quad &+ \frac{1}{2} \left\langle \left[\bar{\zeta}_1, \bar{\zeta}_2 \right]^v, \left[\bar{\zeta}_3, \bar{\zeta}_4 \right]^v \right\rangle \\ &- \frac{1}{4} \left\langle \left[\bar{\zeta}_2, \bar{\zeta}_3 \right]^v, \left[\bar{\zeta}_1, \bar{\zeta}_4 \right]^v \right\rangle - \frac{1}{4} \left\langle \left[\bar{\zeta}_3, \bar{\zeta}_1 \right]^v, \left[\bar{\zeta}_2, \bar{\zeta}_4 \right]^v \right\rangle, \end{aligned}$$

where, for each i , $\bar{\zeta}_i$ is the horizontal lift to $\mathbb{S}^{m(k-1)-1}$ of the vector ζ_i tangent to Σ_m^k . Choose $\{\partial/\partial u_i \mid 1 \leq i \leq m-1\} \cup \{\xi_{i,j} \mid 1 \leq i \leq m, i < j \leq k-1\}$ as the basis of $\mathcal{T}_{\pi(X)}(\Sigma_m^k)$ for $\pi(X)$ in $\Sigma_m^k \cap \pi(\mathbb{X}_{m,k})$. Note that $\partial/\partial u_i$, being a linear combination of the horizontal fields $\partial/\partial \tilde{\lambda}_1, \dots, \partial/\partial \tilde{\lambda}_m$, is already horizontal. Then the only pairs of horizontal vector fields, corresponding to fields from this chosen basis, whose Lie brackets can contribute anything to the Riemannian curvature are among those of the forms $(\partial/\partial u_r, \xi_{i,j})$ and $(\xi_{i_1 j_1}, \xi_{i_2 j_2})$. The expressions for $[\bar{\xi}_{i_1 j_1}, \bar{\xi}_{i_2 j_2}]^v$ are the same as those in the last section with $\tilde{\lambda}_i$

replaced by λ_i and

$$(14) \quad \left[\frac{\partial}{\partial u_r}, \bar{\xi}_{ij} \right]^v = \begin{cases} \left\{ \begin{array}{l} 2\lambda_{r+1}\lambda_j \frac{\lambda_1^2 - \lambda_j^2}{(\lambda_1^2 + \lambda_j^2)^2} \eta_{1j}, & \text{if } r \neq j - 1, \\ 2 \frac{\lambda_1^2 - \lambda_j^2}{\lambda_1^2 + \lambda_j^2} \left\{ 1 + \frac{\lambda_1}{\lambda_1^2 + \lambda_j^2} \right\} \eta_{1j}, & \text{if } r = j - 1, \end{array} \right. & \text{if } i = 1, \\ \left\{ \begin{array}{l} 2u_j \frac{u_j^2 - u_i^2}{(u_i^2 + u_j^2)^2} \eta_{ij}, & \text{if } r = i - 1, \\ 2u_i \frac{u_i^2 - u_j^2}{(u_i^2 + u_j^2)^2} \eta_{ij}, & \text{if } r = j - 1, \\ 0, & \text{otherwise} \end{array} \right. & \text{if } i \neq 1 \end{cases}$$

for $j, r \leq m$. Thus we obtain the Riemannian curvature on $\Sigma_m^k \cap \pi(\mathbb{X}_{m,k})$. In particular we have the formula for the sectional curvature as stated in the following theorem.

THEOREM 5. *The sectional curvatures of $\Sigma_m^k \setminus \pi(\mathcal{S}_{m,k})$, restricted to $\Sigma_m^k \cap \pi(\mathbb{X}_{m,k})$, associated with the distinct pairs of vectors from the chosen basis are all equal to unity save for*

$$K\left(\frac{\partial}{\partial u_r}, \xi_{ij}\right) = 1 + \begin{cases} 3 \frac{\lambda_{r+1}\lambda_j^2}{(1 + \lambda_1)^2(\lambda_1^2 + \lambda_j^2)^2}, & \text{if } r \neq j - 1 \text{ and } i = 1, \\ 3 \frac{1}{(1 + \lambda_1)^2} \left\{ 1 + \frac{\lambda_1}{\lambda_1^2 + \lambda_j^2} \right\}^2, & \text{if } r = j - 1 \text{ and } i = 1, \\ 3 \frac{\lambda_i^2 + \lambda_j^2 - \lambda_r^2}{(\lambda_i^2 + \lambda_j^2)^2}, & \text{if } r = i - 1 \text{ or } j - 1, \\ & \text{and } i \neq 1, \end{cases}$$

$$K(\xi_{ij}, \xi_{rs}) = K(\xi_{ij}, \xi_{sr})$$

$$= 1 + 3 \frac{\lambda_s^2(\lambda_i^2 + \lambda_j^2 - \lambda_r^2)}{(\lambda_i^2 + \lambda_j^2)(\lambda_i^2 + \lambda_s^2)(\lambda_j^2 + \lambda_s^2)}, \quad \text{if } r = i \text{ or } j, s \neq i, j.$$

These results could alternatively be obtained via a general formula of O'Neill that expresses each sectional curvature for the bottom space as the corresponding sectional curvature for the top space *plus an extra nonnegative term*. Thus, quite generally, *Riemannian submersions never decrease the sectional curvatures*.

The component “1 + ” in the above formulae represents the contribution from the top space (a unit sphere) while the remaining (nonnegative) term represents the effect of the submersion.

To compute the Ricci and scalar curvatures of Σ_m^k it is more convenient to take the second approach, so we use the fact that $\mathbf{S}\Sigma_m^k$ is a warped product of \mathbb{R}_+ and Σ_m^k with its metric $d\rho$ determined on $\mathbf{S}\Sigma_m^k \setminus \pi(\mathcal{S}_{m,k})$ by

$$d\rho^2 = dr^2 + r^2 ds^2.$$

We can then use the formulae of O’Neill [56] that relate the curvature of $\mathbf{S}\Sigma_m^k$ to that of Σ_m^k . For this, as already mentioned, the most convenient basis to choose for $\mathcal{F}_{\pi(X)}(\Sigma_m^k)$, where $\pi(X) \in \Sigma_m^k \cap \pi(\mathbb{X}_{m,k})$, is $\{\partial/\partial\lambda_i | 1 < i \leq m\} \cup \{\xi_{i,j} | 1 \leq i \leq m, i < j \leq k - 1\}$.

In the case of the Ricci curvature we obtain the following result, where $d_{mk} = mk - m(m + 1)/2 - 1$ is the dimension of Σ_m^k .

THEOREM 6. *The $d_{mk} \times d_{mk}$ matrix of the components of the Ricci curvature tensor Ric of $\Sigma_m^k \setminus \pi(\mathcal{S}_{m,k})$, restricted to $\Sigma_m^k \cap \pi(\mathbb{X}_{m,k})$, associated with the chosen vector fields has the form $\text{diag}(R_1^*, R_2^*, R_3^*)$. R_1^* is the $(m - 1) \times (m - 1)$ matrix, whose (i, j) th entry $\text{Ric}(\partial/\partial\lambda_i, \partial/\partial\lambda_j)$ is given by*

$$3\lambda_i\lambda_j \left\{ \frac{1}{(\lambda_i^2 + \lambda_1^2)^2} + \frac{1}{(\lambda_j^2 + \lambda_1^2)^2} - \frac{1}{(\lambda_i^2 + \lambda_j^2)^2} + \frac{1}{\lambda_1^2} \sum_{s=2}^m \frac{\lambda_s^2}{(\lambda_s^2 + \lambda_1^2)^2} + \frac{(d_{mk} - 1)}{3\lambda_1^2} \right\}$$

if $i \neq j$, and

$$3 \left\{ 2 \frac{\lambda_i^2}{(\lambda_i^2 + \lambda_1^2)^2} + \sum_{s \neq i} \frac{\lambda_s^2}{(\lambda_s^2 + \lambda_i^2)^2} + \frac{\lambda_i^2}{\lambda_1^2} \sum_{s=2}^m \frac{\lambda_s^2}{(\lambda_s^2 + \lambda_1^2)^2} \right\} + (d_{mk} - 1) \left\{ 1 + \frac{\lambda_i^2}{\lambda_1^2} \right\}$$

if $i = j$; R_2^* is the $m(m - 1)/2 \times m(m - 1)/2$ diagonal matrix, whose $((i_1, j_1), (i_2, j_2))$ th entry $\text{Ric}(\xi_{i_1 j_1}, \xi_{i_2 j_2})$, $1 \leq i_1 < j_1 \leq m$, $1 \leq i_2 < j_2 \leq m$, is zero unless $i_1 = i_2 = i$ and $j_1 = j_2 = j$ when it is

$$\frac{(\lambda_i^2 - \lambda_j^2)^2}{(\lambda_i^2 + \lambda_j^2)} \left\{ (d_{mk} - 1) + 3 \sum_{s=1}^m \frac{\lambda_s^2}{(\lambda_i^2 + \lambda_s^2)(\lambda_j^2 + \lambda_s^2)} \right\};$$

and R_3^* is the $m(k - 1 - m) \times m(k - 1 - m)$ diagonal matrix, whose $((i_1, j_1), (i_2, j_2))$ th entry $\text{Ric}(\xi_{i_1 j_1}, \xi_{i_2 j_2})$, $1 \leq i_1 \leq m < j_1 \leq k - 1$, $1 \leq i_2 \leq m < j_2 \leq k - 1$, is zero unless $i_1 = i_2 = i$ and $j_1 = j_2 = j$ when it is $(d_{mk} - 1)\lambda_i^2$. Evidently the Ricci curvature tensor of $\Sigma_m^k \setminus \pi(\mathcal{S}_{m,k})$ is positive when restricted to $\Sigma_m^k \cap \pi(\mathbb{X}_{m,k})$.

PROOF. On $\pi(\mathbb{X}_{m,k}), \{\partial/\partial\lambda_i | 1 < i \leq m\} \cup \{\xi_{ij} | 1 \leq i \leq m, i < j \leq k - 1\}$ are tangent to $\Sigma_m^k \cap \pi(\mathbb{X}_{m,k})$. Thus, by O'Neill's result for the Ricci curvatures on warped product spaces, the Ricci curvature tensors of $\Sigma_m^k \setminus \pi(\mathcal{S}_{m,k})$ and of $\mathbf{S}\Sigma_m^k \setminus \pi(\mathcal{S}_{m,k})$ are related by

$$\text{Ric}_{\Sigma_m^k}(\zeta_1, \zeta_2) = \text{Ric}_{\mathbf{S}\Sigma_m^k}(\zeta_1, \zeta_2)|_{r=1} + \langle \zeta_1, \zeta_2 \rangle (d_{m,k} - 1) \frac{\langle \text{grad } r, \text{grad } r \rangle}{r^2} \Big|_{r=1},$$

wherever ζ_1 and ζ_2 are vectors tangent to $\Sigma_m^k \setminus \pi(\mathcal{S}_{m,k})$. Hence

$$\begin{aligned} \text{Ric}_{\Sigma_m^k} \left(\frac{\partial}{\partial\lambda_i}, \frac{\partial}{\partial\lambda_j} \right) &= \text{Ric}_{\mathbf{S}\Sigma_m^k} \left(\frac{\partial}{\partial\lambda_i}, \frac{\partial}{\partial\lambda_j} \right) \Big|_{r=1} + (d_{m,k} - 1) \left\langle \frac{\partial}{\partial\lambda_i}, \frac{\partial}{\partial\lambda_j} \right\rangle, \\ \text{Ric}_{\Sigma_m^k}(\xi_{ij}, \xi_{ij}) &= \text{Ric}_{\mathbf{S}\Sigma_m^k}(\xi_{ij}, \xi_{ij}) \Big|_{r=1} + (d_{m,k} - 1) \langle \xi_{ij}, \xi_{ij} \rangle \Big|_{r=1}, \end{aligned}$$

and the components of the Ricci curvature tensor associated with other pairs of the basis of $\mathcal{F}_{\pi(X)}(\Sigma_m^k)$ are zero.

Because the matrix consisting of $\text{Ric}_{\mathbf{S}\Sigma_m^k}(\partial/\partial\lambda_i, \partial/\partial\lambda_j)$ will be $J^t R_1 J$, where R_1 is the matrix in Theorem 4, and J is the $m \times (m - 1)$ Jacobian matrix given by

$$\begin{pmatrix} -\lambda_2/\lambda_1 & -\lambda_3/\lambda_1 & \cdots & -\lambda_m/\lambda_1 \\ 1 & 0 & \cdots & 0 \\ 0 & 1 & \cdots & 0 \\ & & \ddots & \\ 0 & 0 & \cdots & 1 \end{pmatrix},$$

we have

$$\begin{pmatrix} R_1^* & 0 & 0 \\ 0 & R_2^* & 0 \\ 0 & 0 & R_3^* \end{pmatrix} = \begin{pmatrix} J & 0 & 0 \\ 0 & I & 0 \\ 0 & 0 & I \end{pmatrix}^t M_{m,k} \begin{pmatrix} J & 0 & 0 \\ 0 & I & 0 \\ 0 & 0 & I \end{pmatrix} + (d_{m,k} - 1) G_{\Sigma_m^k},$$

where $G_{\Sigma_m^k}$ is the matrix of the metric on Σ_m^k derived from (5), and $M_{m,k}$ is the matrix of the components of the Ricci curvature tensor of $\mathbf{S}\Sigma_m^k \setminus \pi(\mathcal{S}_{m,k})$ in Theorem 4, with the $\tilde{\lambda}_i$ replaced by λ_i . This proves the theorem. \square

COROLLARY. The scalar curvature of $\Sigma_m^k \setminus \pi(\mathcal{S}_{m,k})$ is equal to the sum of the scalar curvature of $\mathbf{S}\Sigma_m^k \setminus \pi(\mathcal{S}_{m,k})$ (with the $\tilde{\lambda}_i$ replaced by λ_i) and an extra term $d_{m,k}(d_{m,k} - 1)$.

Thus the scalar curvature is bounded below by $d_{m,k}(d_{m,k} - 1)$ and is (positively) infinite at the singularities.

PROOF. This follows from a result on warped products in O'Neill's book [56] which implies that the relation between the scalar curvatures $S_{\mathbf{S}\Sigma_m^k}$ of

$S\Sigma_m^k \setminus \pi(\mathcal{S}_{m,k})$ and $S_{\Sigma_m^k}$ of $\Sigma_m^k \setminus \pi(\mathcal{S}_{m,k})$ is

$$S_{\Sigma_m^k} = \left\{ S_{S\Sigma_m^k} + \frac{d_{m,k}(d_{m,k} - 1)}{r^2} \right\} \Big|_{r=1}. \quad \square$$

In the simplest case Σ_3^4 when $m = 3$ and $k = 4$ the above formula can be reexpressed in a particularly neat form, and it will be convenient to divide this by $d_{m,k}(d_{m,k} - 1)$ (here equal to 20, because $d_{3,4} = 5$) so as to obtain an expression for the ‘‘average’’ sectional curvature. We then have

$$(15) \quad \text{average}(K) = 1 + \frac{3}{10} \frac{1 + 2(\lambda_2^2\lambda_3^2 + \lambda_3^2\lambda_1^2 + \lambda_1^2\lambda_2^2)}{(\lambda_2^2 + \lambda_3^2)(\lambda_3^2 + \lambda_1^2)(\lambda_1^2 + \lambda_2^2)},$$

where $\lambda_1 \geq \lambda_2 \geq |\lambda_3|$ and $\lambda_1^2 + \lambda_2^2 + \lambda_3^2 = 1$.

Thus, for all shape spaces, *average(K) is never less than unity and explodes to infinity in the neighbourhood of each singularity (i.e., when λ_2 and therefore also λ_3 tends to zero).*

This last expression for the scalar curvature of the special shape space Σ_3^4 was derived about 1981 by Kendall using an ad hoc method, now lost. Contour lines for *average(K)* (drawn on a hemisphere of $\lambda_1^2 + \lambda_2^2 + \lambda_3^2 = 1$) will be found in his contribution to the discussion following Bookstein’s paper ([4], page 223).

8. Three applications. We now return to the three examples mentioned in the first section of this paper.

8.1. *Shapes of fossils.* This problem arose when James Crampton of the Department of Earth Sciences in Cambridge asked us if we could suggest a technique that would assist in the classification of shapes of fossil specimens from the genus *Inoceramus*. We were encouraged to concentrate on the outer boundary of a plane projection of each fossil, starting at the outer extremity of the hinge line, and then moving along this and around the boundary of the shell until the outer extremity of the hinge line was again reached. For each of 12 specimens he gave us the coordinates of 24 equally-stepped points on this boundary (obtained with the aid of a digitiser). In this way each specimen was identified with a point in the shape space $\Sigma_2^{24} = \mathbb{C}P^{22}(4)$, and the whole data set was thus represented by 12 shapes identified with points in that 44-dimensional shape space. We decided to proceed as follows.

(a) We first calculated the *geodesic* intershape distances δ for the ${}^{12}C_2 = 66$ distinct pairs of shells. These determine the off-diagonal values in a 12×12 symmetric distance-matrix. The geodesic distances were computed by using the special techniques first introduced by Le [49].

(b) Now a geodesic distance in shape space measures *shape-dissimilarity*, while what we need for correspondence analysis is *shape-similarity*. We therefore replace the geodesic distance s by $(1 - \sin s)^4$, this being an empirical

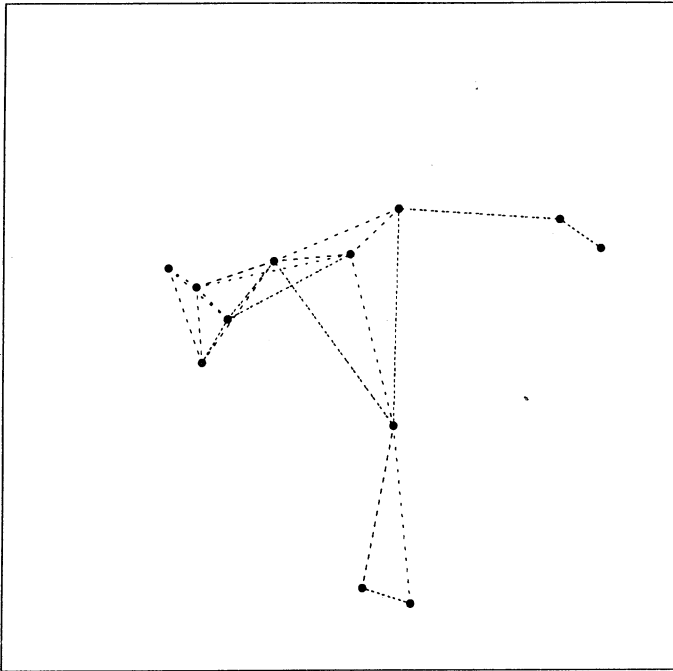


FIG. 1. A 2D correspondence analysis plot for the fossil data.

antimonotone rescaling that happens to produce a reasonably uniform distribution of similarity values. Note that the diagonal entries in the matrix will all be equal to unity.

(c) We then performed a standard correspondence analysis as explained for example in Hill's paper [19].

(d) We examined the first three nontrivial eigenvectors produced by the correspondence analysis procedure and plotted for each shell-shape its position in two dimensions as specified by the first two such normed eigenvectors (Figure 1). In that picture links are drawn between those pairs of shapes that are separated by relatively small geodesic distances. It will be seen that we obtain a plot consisting of three "branches" spreading out from a common central region.

(e) It was feared that the use of a merely two-dimensional projection might have concealed important detail, and so we also constructed a computer-drawn stereo plot making use of all of the first three nontrivial eigenvectors (Figure 2).

This stereo option is now one of the standard components of DGK's correspondence analysis program. Readers with normal vision may be able to "fuse" the pair of stereo views by observing the left-hand plot with the left eye and vice versa, but the use of a stereo viewer is in general recommended.

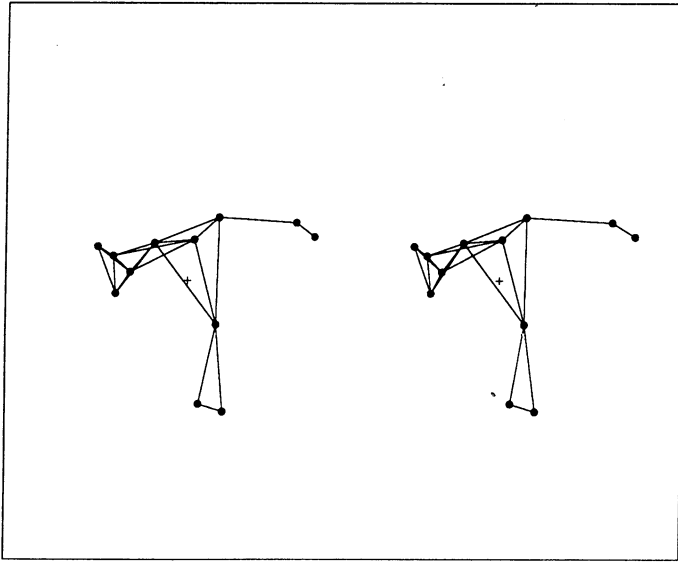


FIG. 2. A 3D stereo correspondence analysis plot for the fossil data.

Notice that in each component of the stereo plot the centroid is marked by a “+” sign. It proves helpful in naked-eye viewing to start by fuzing these two “+” signs, and once that is done the three-dimensional view of the whole configuration should be apparent.

The stereo view makes clear the genuine separation between the three “branches.”

A final plot Figure 3 is similar to Figure 1 but now shows at each locus a size-standardised portrait of the corresponding shell outline itself, thus facilitating visual assessment in relation to the original data.

8.2. *Collinearity-testing.* We turn next to the “collinearity” problem in Section 1, and make use of data studied by Broadbent [5] concerning 52 “standing stones” in Cornwall. This data-set has also been analysed by Kendall and Kendall [37]. In these two earlier investigations the methods used were quite different from that now to be described.

In the present investigation we decided to confine our attention to four-point collinearities. Now four labelled points in \mathbb{R}^1 that are not totally coincident determine a shape that can be identified with a point on the sphere $\Sigma_1^4 = \mathbb{S}^2(1)$, while four labelled (and again not totally coincident) points in \mathbb{R}^2 determine a shape that can be identified with a point on the complex projective space $\Sigma_2^4 = \mathbb{C}\mathbb{P}^2(4)$.

If the points in this last tetrad happen to be exactly (or nearly) collinear, then the shape-point in $\mathbb{C}\mathbb{P}^2(4)$ will lie on (or near) the “equator” of the complex projective space. That “equator” is, in fact, the *real* projective space

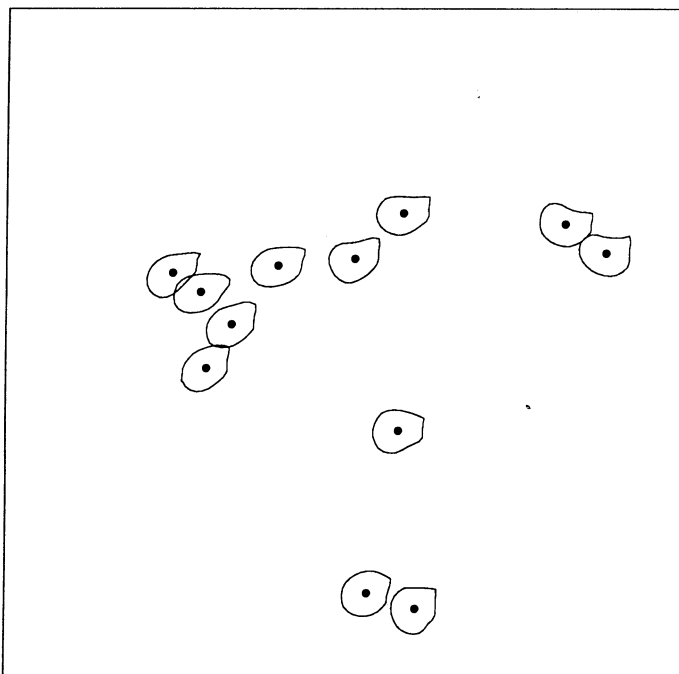


FIG. 3. The 2D correspondence analysis plot with the fossil profiles shown.

$\mathbb{RP}^2(1)$. This projective two-sphere of unit radius is thus the natural home for the shapes of *exactly* collinear labelled tetrads in \mathbb{R}^2 .

If we now pick out from our two-dimensional data set a *nearly* collinear tetrad ABCD represented by a point P in the four-dimensional projective sphere, then P will be close to some “nearest point” Q on the projective two-sphere, and we can regard Q as identifying the shape of the truly collinear tetrad which best approximates the original tetrad in \mathbb{R}^2 , so we can use the length δ of the shortest geodesic arc from P to Q as a measure of *the degree of noncollinearity of the labelled set ABCD of four points in \mathbb{R}^2* . This is an intuitively attractive procedure, and we shall see that there is a sense in which it is also the statistically natural one.

In a practical context the labelling of the four points will only be of secondary importance. The projective two-sphere can be dissected into 24 regions (which turn out to be 24 congruent spherical triangles) that match the 24 possible labellings. (Because we shall only be interested in near-collinearities, we can without ambiguity suppose that the points of the tetrad are labelled as A, B, C, D following their order along their best-fitting straight line.) Figure 4 will help to illustrate the situation. Note the small triangular markers that locate the shapes of the *equispaced* collinear tetrads.

The three corners of any one of these spherical triangles (say the spherical triangle for which the order of the labelling is (A, B, C, D)) will then represent

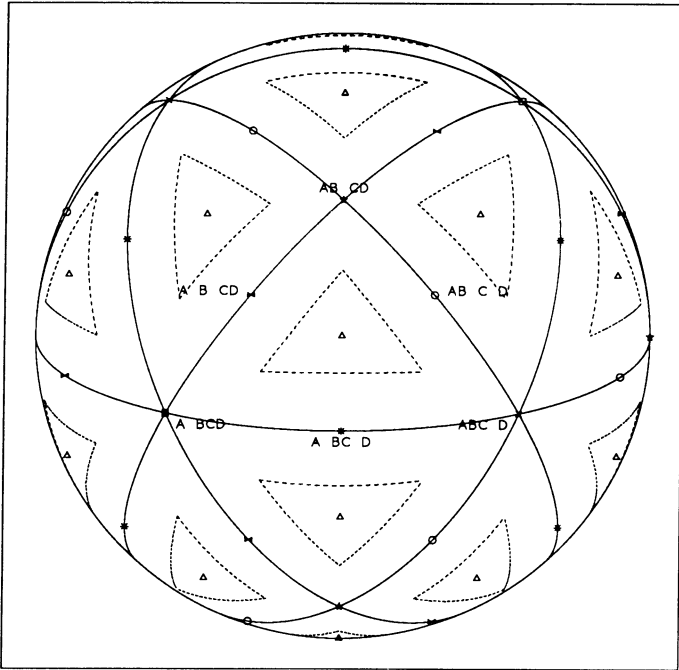


FIG. 4. $\mathbb{R}P^2$ seen as a sphere, with the 24 "tiles."

the three possible double-coincidence situations:

$$(A \ BCD), \quad (AB \ CD), \quad (ABC \ D).$$

The midpoints of the sides will correspond to the single-coincidence situations:

$$(A \ B \ CD), \quad (A \ BC \ D), \quad (AB \ C \ D),$$

while the central point of that spherical triangle will represent the equispaced tetrad

$$(A \ B \ C \ D)$$

identified in Figures 4–6 by the small triangular marker.

Now for distributional (but not metrical) purposes the equal-area projection of $\mathbb{R}P^2(1)$ onto a right-circular cylinder can be used as an alternative to $\mathbb{R}P^2(1)$ itself, and further we can confine our attention to the image on that cylinder of just *one* of the "spherical tiles"—say the one just referred to that has ABCD as the ordering of its points.

Figure 5 illustrates the map onto the cylinder, while Figure 6 shows an enlargement concentrating on the "central" tile and containing further detail that we will describe in a moment.

We now have to call on the theory developed in Le [50], where it is shown that generically there is a unique shortest geodesic arc from a point P in $\Sigma_2^4 = \mathbb{C}P^2(4)$ to the unique nearest point Q in the "equatorial set" $\mathbb{R}P^2(1)$, and

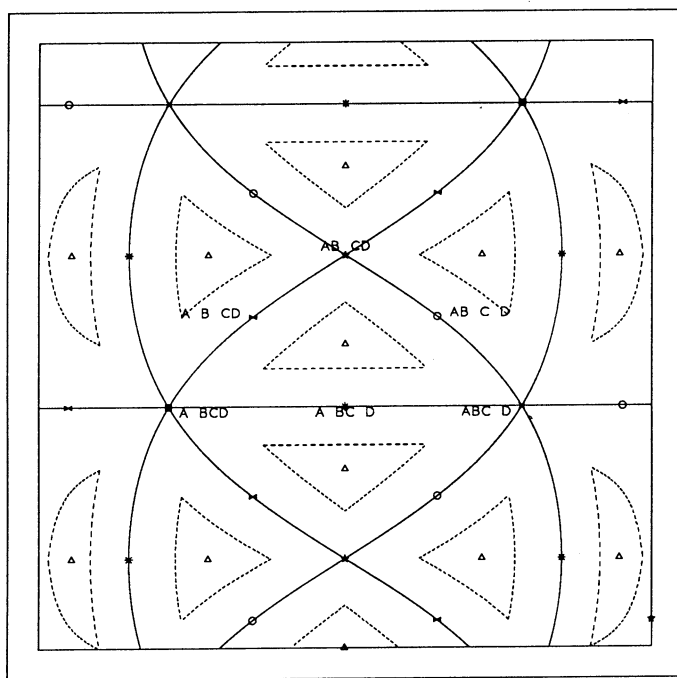


FIG. 5. The equal-area projection of $\mathbb{R}P^2$ onto a cylinder (opened out).

where techniques for *finding* Q and *evaluating* the geodesic distance d from P to Q are both worked out in detail. We must refer the reader to Le's paper for these technicalities, and especially for her method for computing d . In Kendall [26] and Le [50] it is shown that, for a random tetrad in two dimensions generated by iid sampling from a Gaussian distribution with circular symmetry, the quantity $\delta = \sin^2(2d)$, has the uniform distribution on $[0, 1]$. This fact suggests that it will be convenient in what follows to work with the monotone transform $\delta = \sin^2(2d)$, $0 \leq d \leq \pi/4$, rather than with d itself, and accordingly we shall do this. (Note that $\pi/4$ is the maximum possible value of d . See [26].) Now we are interested here not in exact collinearities, but in *near-collinearities*. The degree of nearness δ that is to be regarded as critical must be decided upon by the initiator of the investigation. It is in fact desirable to choose two such "levels of nearness." The first (and strictest) δ_1 ($= 0.00001$) is used to define really remarkable near-collinearities, while the second (and weakest) δ_2 ($= 0.001$) is used to provide a standard for comparison. We recommend plotting those tetrads that satisfy the strict requirement as large solid black spots, and those that are to provide the background comparison as small crosses. The result of this procedure for the Broadbent data-set will be seen in Figure 6.

It is, of course, the large solid black spots that are of primary interest: They are *candidates for meaningful four-point collinearities*. The small crosses

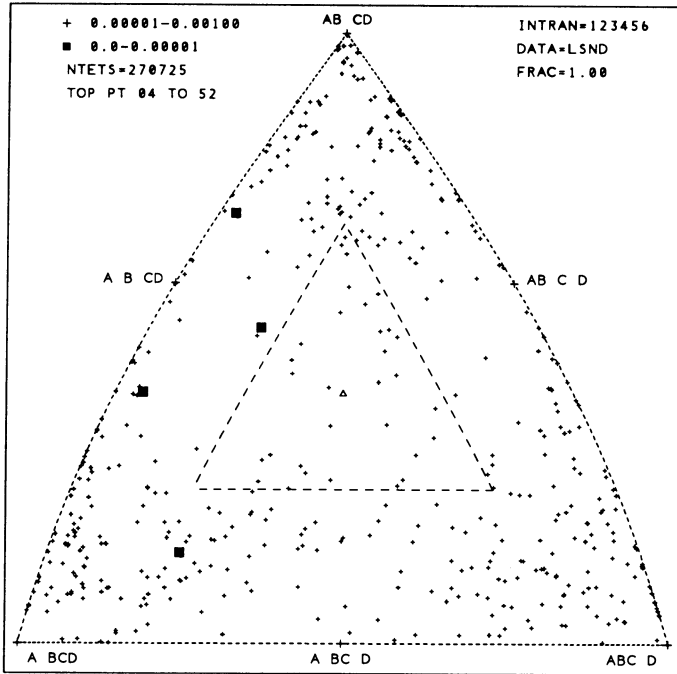


FIG. 6. *The central tile (enlarged, with Land's End data).*

representing other less remarkable collinearities provide essential background information and also supply a check on the methodology.

However this is not quite all. We must take care to distinguish “well spaced-out” solid-spot collinearities from those that have two or more nearly coincident member-points, because configurations of the latter type will normally be dismissed as three-point collinearities that just happen to have a nearly-replicated member-point. A useful criterion for this purpose is the rather artificial requirement

$$\min(AB, BC, CD) \geq AD/5.$$

The choice of the number 5 in this formula is somewhat arbitrary, and may well need to be altered. This convention allows us to exclude *all large solid black spots that are too close to the boundary (or corners) of the basic spherical triangle* (all the points of which represent *exact* single or double degeneracies).

In Figure 6 the locus corresponding to the “critical” situation (equality in the above formula) is shown as a *dotted* triangle whose edges correspond, in fact, to arcs of certain other spherical triangles on the original $\mathbb{R}P^2$ along which the inequality reduces to an equality (cf. Figures 4 and 5).

To sum up, the “large solid black spots” mark the strikingly close collinearities, characterised by a very small length of the “geodesic perpendicular” from the original shape-point onto the exact-collinearity locus, *but such points*

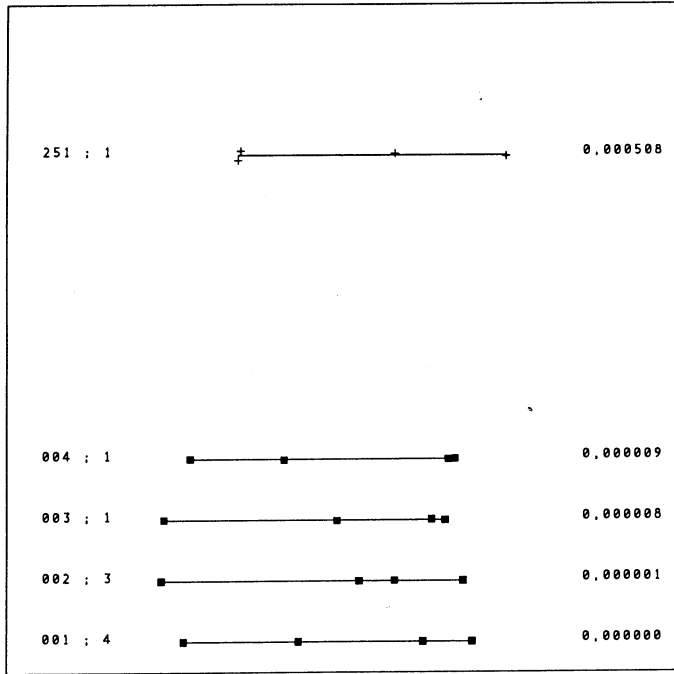


FIG. 7. The first four (and the 251st) most nearly collinear Land's End tetrads.

are to be discounted when they lie on the edge of or outside the inner dotted triangle.

For the Broadbent data it turns out that none of the large solid black spots lie within the inner dotted triangle that would (on this criterion) contain the genuine near-collinearities if there were any—though one large solid black spot is indeed a “near miss.”

A considerable advantage of plots such as Figure 6 is that we see the way in which the collinearity-criterion is actually working, instead of having to rely on a merely numerical judgement. Because the inequality-criterion and its geometric equivalent is of a somewhat arbitrary form, it is helpful to supplement the graphical output by an additional plot or plots showing some of the more nearly collinear tetrad-configurations themselves—say all of those corresponding to the large solid black spots, together with some of those (corresponding now to small crosses) that have a δ -value not more than say $50\delta_1$. Figure 7 shows a plot of this sort for the Broadbent data. (The straight-line segments in this diagram are determined by singular-values decomposition.)

From a classical Fisherian point of view we could say that the size and shading of the spot representing the quantised δ -value in the graphical representation is the basic *test statistic*, and that its distance from the edge-or-exterior of the inner triangle is the associated *ancillary statistic*. Thus a natural differential-geometric analysis has led us from the initial description of

the problem to an extension of classical testing procedures in a novel curved-space context.

Diagrams such as Figure 6 reveal a great deal of further information that cannot be discussed in full detail here. Thus the reader may have noticed the strings of small crosses hugging the left-hand and right-hand "arches" bounding the larger spherical triangle. These signal the presence of "close pairs" in the data set. Obviously if the site of a "close pair" happens to be nearly collinear with two other points, then such a "boundary" point will appear in the diagram.

The interpretation of such phenomena is not always self evident, and experimentation with a number of artificial *and real* data sets is strongly recommended. It is also very helpful to have available as many different graphical presentations of the data as possible, and we now exhibit a few of these.

Figure 8 shows a scatter-plot for $\max(\angle ABD, \angle ACD)$ (vertical axis) against δ (horizontal axis). This plot shows in a very striking way the complete inadequacy of the usual max-angle criterion as a collinearity statistic.

Figure 9 shows the geographical locations of the 52 Broadbent points, together with the four four-point collinearities that correspond to the four "large solid black spots." It is a striking fact that two of these four collinearities each has *five or more well separated points on or near it*.

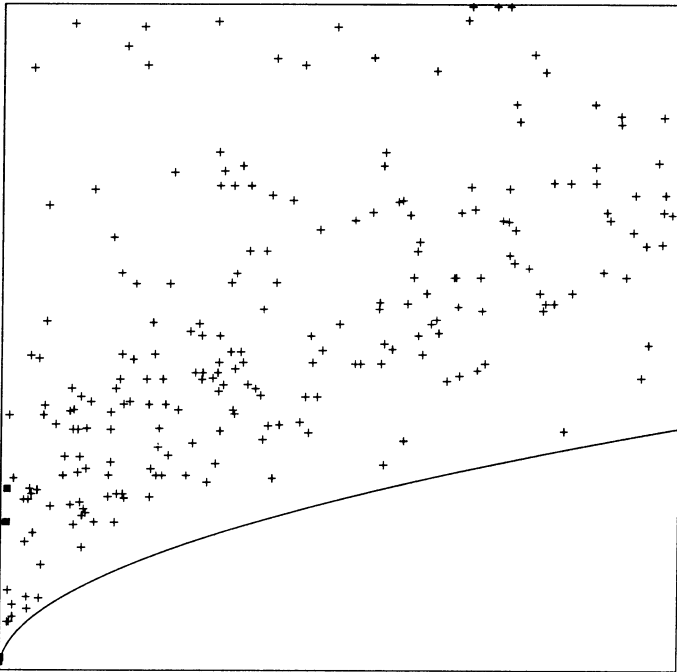


FIG. 8. *The angular criterion plotted against the shape-theoretic criterion.*

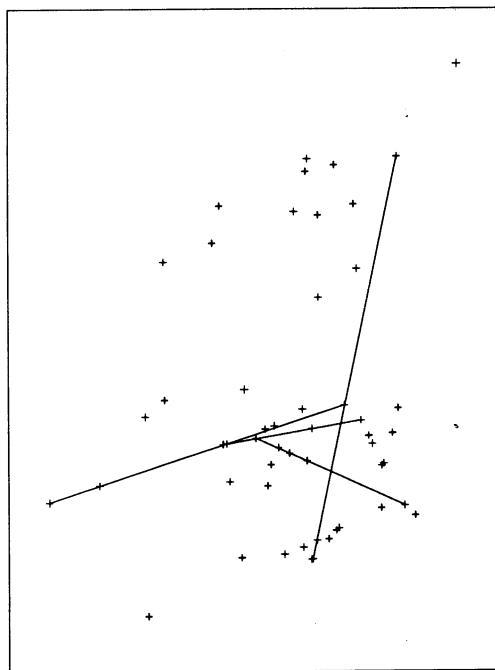


FIG. 9. *Broadbent's Land's End data, with the four best collinearities.*

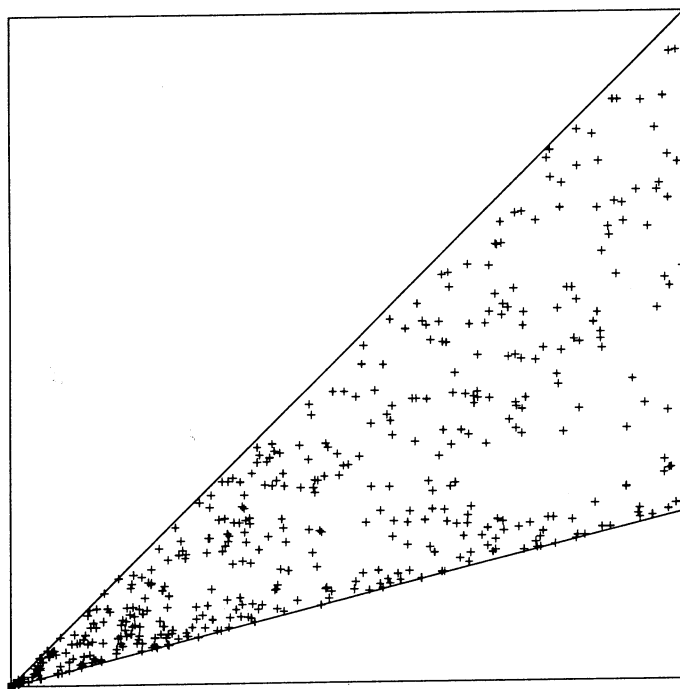


FIG. 10. *A "flat-space" criterion compared with the shape-theoretic criterion.*

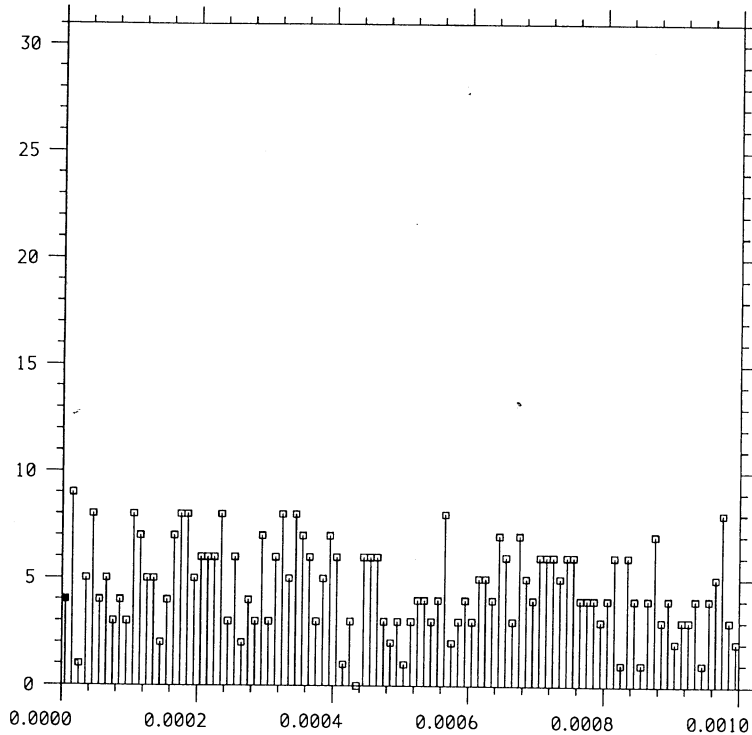


FIG. 11. Histogram of the 100 most nearly collinear tetrads.

Figure 10 compares the δ -value derived here from shape-theoretic considerations (horizontal axis) and a similar but more classical criterion (vertical axis) derived by fitting a straight line in 2D and measuring the lateral departures from that. Here (in contrast to Figure 8) the two techniques are obviously trying to measure the same thing, but instead of a linear relationship we have points scattered within a wedge whose upper boundary is about 4 times as large as the lower boundary. This factor 4 quantises the penalty to be paid if one uses a crude linear analysis instead of the shape-theoretic one.

Finally Figure 11 shows a histogram of the shape-theoretic δ -values for the range $0 \leq \delta \leq 0.001$. This picture shows that there is nothing out of the ordinary at the small- δ end of the range. The only really striking feature of the Broadbent data set is the pair of *multiple* collinearities noted above. (This comment of course largely echoes Broadbent's own conclusions.)

Figures 4, 5, and 6 were first published in a contribution to a Royal Statistical Society Discussion Meeting (Kendall [33]), and are reproduced here by permission of the Society.

8.3. *Shapes of Poisson-Delaunay tetrahedra.* Our third and last problem is concerned with the shapes of the polyhedral cells in a Voronoi tessellation in

three dimensions generated by a three-dimensional homogeneous Poisson process. Now the dimensionality is not in itself a problem (though here we shall confine ourselves to three dimensions), nor does it matter that the polyhedral cells carry no specified labelling because we can always impose an arbitrary labelling and quotient it out at the end of the calculation. The difficulty lies in the fact that we have not yet investigated the fraction of shape space that is characterised by the special condition (an essential feature of Voronoi cells) that *each labelled point is an effective vertex* (i.e., each such point lies properly outside the convex hull of all the others). Until this situation is thoroughly explored (and it presents a very attractive problem) it would be premature to invest too much effort in the shape analysis of Voronoi cells.

However, there is a useful duality between Voronoi tessellations and Delaunay tessellations, and happily with Delaunay tessellations generically each vertex does lie properly outside the convex hull of all the other vertices. What is more, generically each Delaunay cell is an $(m + 1)$ -simplex when the tessellation lives in \mathbb{R}^m . Here again there is no preferred labelling of the vertices, but this is not a problem if we agree to impose an arbitrary labelling and then quotient it out at the end. We therefore discuss the Delaunay problem, and leave the Voronoi problem for another occasion. *We shall assume throughout that the set of points generating the tessellation is a homogeneous Poisson process.*

The two-dimensional case has already been fully explored (Kendall [25, 30, 31]), and so we concentrate here on dimension $m = 3$.

A key contribution to the solution will be the following theorem for general m that was established in a more general context in the papers just cited.

Let us write R for the radius of the circumsphere of an m -dimensional simplex in \mathbb{R}^m , and let us write L for the square root of the sum of the squares of the distances $|P_i G|$ from the vertices P_i to their centroid G . Now suppose that we have available an infinite sequence of independent standard Gaussian simplexes in \mathbb{R}^m . [This means that the simplexes are to be independent, and that for each individual simplex the $m + 1$ vertices are to be iid Gaussian with a unit isotropic variance matrix and a common mean $(0, 0, \dots, 0)$.] For each such simplex calculate the value of the random variable

$$\tau = (R/L)^{m^2} (m + 1)^{m^2/2}, \quad 1 \leq \tau < \infty.$$

Then if we accept that simplex when $\tau U \leq 1$, and reject it when $\tau U > 1$, respectively, where the independent U -variables are to be drawn from the distribution $\text{unif}[0, 1]$, *the accepted simplexes will form an infinite sequence of independent Poisson–Delaunay simplexes in \mathbb{R}^m .*

Thus when $m = 3$ we can easily generate as many independent Poisson–Delaunay tetrahedra as we please, and in this way can study the distribution of their shapes in the shape space Σ_3^4 . That is the programme we here propose to carry out. We shall want to illustrate the results graphically, and this will involve some ingenuity because the shape space Σ_3^4 is five-dimensional.

Now the shape of any one Poisson–Delaunay tetrahedron can be adequately described by the diagonal matrix $\Lambda = (\lambda_1, \lambda_2, \lambda_3)$ together with the (right-hand) rotation matrix $V \in \mathbf{SO}(3)$. [Note that we can take V to lie in $\mathbf{SO}(3)$ rather than in $\mathbf{O}(3)$ because we have left λ_3 free to assume either sign.] Evidently we can display all the “ λ ” information in a (λ_3, λ_1) diagram. This loses no information about Λ because

$$\lambda_2 = +\sqrt{(1 - \lambda_3^2 - \lambda_1^2)}.$$

We shall call the region available to (λ_3, λ_1) the *basic region*. It corresponds to a spherical triangle with angles $(\pi/2, \pi/3, \pi/3)$ that is a totally geodesic submanifold of the “top” space which maps bijectively onto a totally geodesic submanifold of the “bottom” space (the shape space Σ_3^4). (The proof of that statement is just the observation that in the top space the preshape point moves in a direction orthogonal to the fibre whenever the λ 's are perturbed.)

We can plot the point $(\lambda_1, \lambda_2, \lambda_3)$ directly onto the sphere $\mathbb{S}^2(1)$ (or rather, the appropriate spherical triangle thereof), but in many circumstances (and in particular, here) it is more convenient to plot (λ_3, λ_1) (which contains all the λ -information) via a suitable rotation of the sphere and the classical equal-area projection from $\mathbb{S}^2(1)$ onto a convenient snugly-fitting cylindrical sleeve, which is then cut along a suitable generator and opened out.

With a suitable choice of axes this yields a plotting-region that is a curved isosceles triangle looking rather like a bell. A vertical axis of symmetry (the λ_1 -axis) cuts the base orthogonally, and passes through $(1, 0, 0)$ (the home of the singularities) and the point $(1/\sqrt{2}, 1/\sqrt{2}, 0)$. The λ_3 -axis cuts that axis orthogonally at the last mentioned point, and runs from $(1/\sqrt{3}, 1/\sqrt{3}, -1/\sqrt{3})$ (the negatively oriented regular simplex) to the complementary point in which the last coordinate is positive (the positively oriented regular simplex).

However this λ -representation takes no account of the shape-variables associated with the rotation matrix V , and in order to plot at least a quantised version of the V -information we now choose and dissect an appropriate coset of the group $\mathbf{SO}(3)$ and distinguish 24 abutting but nonoverlapping “compartments” into which it can naturally be subdivided.

This “quantisation” can be carried out in many different ways, and we choose the one that follows. We record the signs of the nine elements of the matrix V , and observe that it is permissible and *appropriate* (if needed) to borrow diagonal rotations in $\mathbf{SO}(2)$ from the rotation matrix U in $\mathbf{SO}(3)$ that lies to the left of Λ in the singular-values decomposition and to use these (i) to switch the signs in the first and third rows of V and then (ii) to switch the signs in the second and third rows of V in such a way that each of v_{11} and v_{21} becomes nonnegative.

This leaves us with a standardised V having two fixed (nonnegative) signs in the positions $(1, 1)$ and $(2, 1)$, and seven variable signs elsewhere in the matrix.

Now because we are dealing with a rotation matrix these seven variable signs are by no means arbitrary. There are in all just four possibilities for the

signs of (v_{12}, v_{13}) , and these are each individually to be combined with just three possibilities for the signs of v_{22} and v_{23} , giving so far 12 possible variable-sign combinations. In addition we have an additional factor from the (now rather limited) sign-possibilities in the bottom row. It turns out that *this extra factor is in fact equal to 2*.

To see that this is so, note that the third row is the vector product of the first two rows. Careful examination of the possibilities then shows that two (not always the same two) of the elements in the third row have signs that are already determined, while the third sign in that row is free. Thus, on putting all this together, we have proved the nice little lemma that *the so standardised V matrix has exactly 24 possible sign patterns*.

We can now use these 24 possibilities for the sign pattern in the standardised version of V to cut up the chosen coset of $\mathbf{SO}(3)$ into 24 “compartments” that do not overlap but may share common boundaries.

We then replace the shape space by an approximation that is the Cartesian product of (1) the bell-shaped area-true projection of the spherical triangle carrying the variables $(\lambda_1, \lambda_2, \lambda_3)$ and (2) the 24-point discrete space that now represents the chosen coset of $\mathbf{SO}(3)$.

This means that if we construct a diagram consisting of 24 replicates of the “bell,” each identified with one of the 24 possible sign patterns, then *we will be able to “see” the five-dimensional shape space modulo the approximation being used*, and so to enjoy a direct, if approximate, perception of “what lies where” in five dimensions. We have carried out this programme in full, and now present two examples of its use.

In the first example we constructed 8000 independent tetrahedra with iid standard *Gaussian* vertices (Figure 12). Notice the bilateral symmetry in each “bell,” and the falling-off of the density towards zero at the edges (and especially at the vertices) of the “bell.”

In the second example we made use of Kendall’s device mentioned above that enables one by optional selection (utilising the size-standardised version $\rho = R/L$ of the circumradius R) to select from an iid sequence of Gaussian tetrahedra a subsequence that is again iid and whose members are Poisson–Delaunay tetrahedra. We can then construct Figure 13, which allows one to “see” in the five-dimensional shape space how the shapes of these 8000 iid Poisson–Delaunay tetrahedra are distributed.

(Of course what one does in practice is to prepare to create sequentially some 80,000 Gaussian tetrahedra, and then to abandon the construction as soon as 8000 Poisson–Delaunay tetrahedra have been obtained.)

The reader will notice the almost vacant vertical medial strip lying below the uppermost vertex in each bell in Figure 13. This feature is easy to explain. It simply reminds us that Poisson–Delaunay tetrahedra are very unlikely to be even approximately plane, the point being that the medial vertical line in each bell is the locus of the degenerate (plane) tetrahedral shapes (with a near-infinite value of ρ).

Another very interesting feature of Figure 13 is that the 8000 Poisson–Delaunay points are approximately equi-frequently distributed among the 24

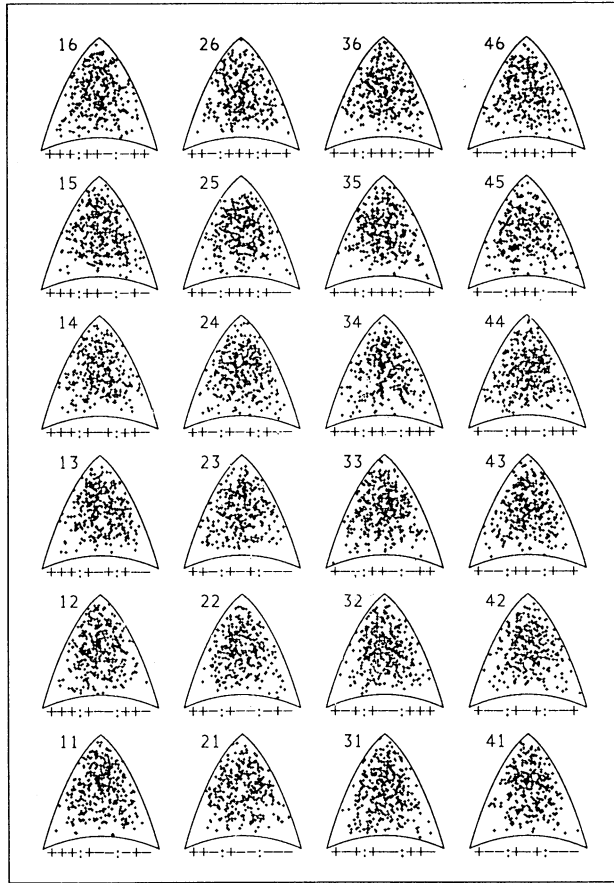


FIG. 12. The "bell" plot for the shapes of 8000 Gaussian tetrahedra.

bells. The corresponding feature in Figure 12 merely reflected a well known property of the singular-values decomposition of a Gaussian matrix, but its repetition in Figure 13 came as a surprise to us. It suggests several interesting possibilities that we hope to explore on another occasion.

The ratio of the number of Poisson–Delaunay tetrahedra obtained to the number of Gaussian tetrahedra used was 0.18613. The theoretical value for this ratio in an infinite sample is 0.14726... The program took about 7 seconds to create each 1000 Poisson–Delaunay tetrahedra, and that rate could be improved upon by cutting out the large volume of ancillary diagnostic material requested by this exploratory program.

It is important to stress here the quite different behaviour of Poisson–Delaunay tessellations that are based on a given *finite* set of points. In that case we have to take into account what happens near the boundary. A substantial proportion of the boundary tiles will be "outward looking," with large circumspheres that succeed in being void precisely because they *are* at

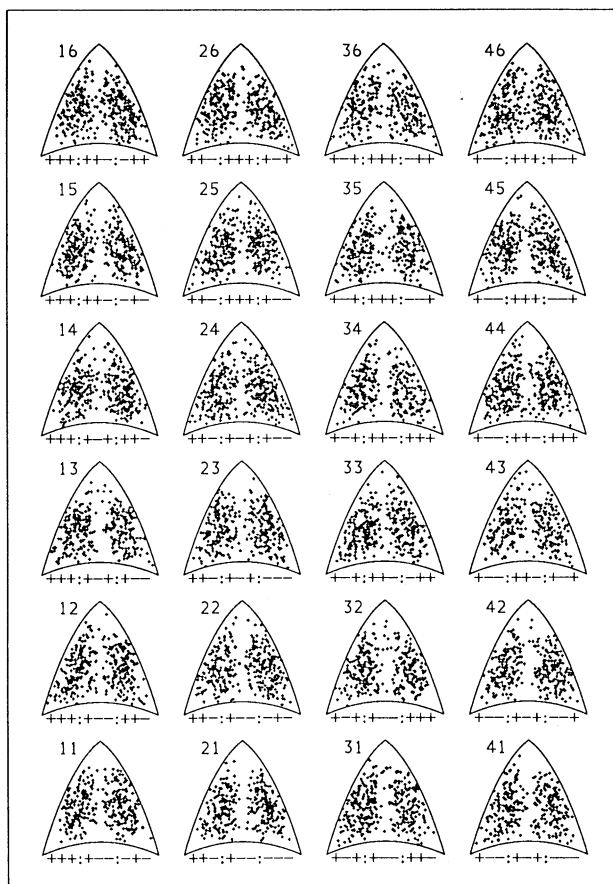


FIG. 13. The “bell” plot for the shapes of 8000 Poisson–Delaunay tetrahedra.

the boundary, and so the analogous plots for such a finite situation will tend to have the typical Poisson–Delaunay void along the median line “filled in” by contributions from boundary tiles. The quantitative aspects of this remark could be sketched on an asymptotic basis, but we will not do that here.

To conclude this discussion we wish to comment informally on the nature of a so-called “duality” between infinite Poisson–Delaunay and Poisson–Voronoi tessellations of \mathbb{R}^m . Here the true “duality” hinges rather on the relationship between the collection of *all the Delaunay tiles that meet at a given vertex*, and the collection of *all the faces of a single Voronoi tile*. Thus if we wish to discuss the shape of an individual Voronoi tile then we are confronted with a problem as hard as that of describing the whole “fan” of Delaunay tiles that meet at a common point.

A little is known about such “fans” (Kendall [30, 31]). The number of Delaunay tiles meeting at a given point grows fantastically quickly with

increase in the dimension m , and there will be about 44 million million such tiles when $m = 15$. Very little is known about the statistical distribution of the Delaunay hypersolid angles that have a vertex at a given Poisson point in \mathbb{R}^m , even for $m = 3$, but we conjecture that it will consist asymptotically of a relatively few “chunky” hypersolid angles accompanied by a vast multitude of “needle-like” ones. Note however that these “needles” will *not* normally have a large circumradius.

Arguing by duality one would expect for a high-dimensional Voronoi tile a moderate number of large faces supplemented by a vast multitude of minute faces.

Is this correct? It seems reasonable, but an attempt to confirm it by a numerical simulation is at present held up by the difficulty of computing hypersolid angles in many dimensions. We are, of course, familiar with the apparatus constructed by Schläfli for such purposes, but we would welcome advice about its use.

To conclude this discussion we mention here that the procedure for “viewing” what goes on in the five-dimensional shape space can also be used dynamically with great effect. Specifically, we can produce in this way, for ready visual examination, (a) *the global behaviour of one or more geodesics*, and (b) *the global behaviour of the paths of Brownian motions (or any other diffusions)* in Σ_3^4 . We hope to study such possibilities in a sequel to this paper.

We also have in mind the analogous problems associated with Σ_m^k when k and m are general. Obviously further detail has to be sacrificed when m is equal to 4 or more, and a reasonable strategy would be to replace $(\lambda_1, \dots, \lambda_m)$ by $(\lambda, \lambda_{m-1}, \lambda_m)$, where

$$\lambda = +\sqrt{(\lambda_1^2 + \dots + \lambda_{m-2}^2)}.$$

In principal the standardisation and decomposition of the Stiefel manifold that now replaces $\mathbf{SO}(3)$ could be done on a sign-pattern basis as before, but the number of distinct sign-patterns would become uncomfortably large and it seems likely that some further amalgamation would be necessary—especially for large k .

8.4. The importance of global considerations. We close this paper with a general remark that seems to us important. The three applications that we have described all depend in different ways on the *global* geometry of the relevant shape spaces. In the first two applications we only needed the shape spaces $\Sigma_1^k = \mathbb{S}^{k-2}(1)$ and $\Sigma_2^k = \mathbb{CP}^{k-2}(4)$, for each of which the global metric geometry is thoroughly understood. But in our third application involving Σ_3^4 we were in quite a new geometric environment, and had to investigate its (previously unknown) global metric structure in some detail before we could adequately deal with the problem under discussion.

It seems clear that this pattern will be the norm whenever we are concerned (as there) with an ambient dimension m that is greater than or equal to 3. We already have an adequate study of the geodesic geometry (Le [49, 50]), and

work on the homology structure (Barden [3] and Kendall [36]) is well advanced. This may not suffice for all the applications, and more ambitious global investigations (for example involving homotopy) are being planned. Perhaps they will be needed.

Acknowledgments. We have benefited greatly from the comments and suggestions of our colleagues Dennis Barden, Marjorie Batchelor, Keith Carne and Wilfrid Kendall, and we also wish to thank the referees who encouraged us to enlarge the paper by adding an account of some substantial applications.

We also wish to acknowledge support from Darwin and Gonville and Caius Colleges in Cambridge and from the Science and Engineering Research Council.

Note. We have attempted to construct a general bibliography for shape theory and some of its applications, and not all of the papers listed here are referred to in the text. The reader is advised to consult in addition the complementary bibliography in the monograph by Rohlf and Bookstein [59], which is particularly concerned with biological applications.

REFERENCES

- [1] AMBARTZUMIAN, R. V. (1982). Random shapes by factorisation. In *Statistics in Theory and Practice* (B. Ranney, ed.). Swedish Univ. Agric. Sci., Umea.
- [2] AMBARTZUMIAN, R. V. (1990). *Factorization Calculus and Geometric Probability*. Cambridge Univ. Press.
- [3] BARDEN, D. (1993). Decomposing the chain-complex for shape spaces. Unpublished manuscript.
- [4] BOOKSTEIN, F. L. (1986). Size and shape spaces for landmark data in two dimensions (with discussion). *Statist. Sci.* **1** 181–242.
- [5] BROADBENT, S. R. (1980). Simulating the ley hunter (with discussion). *J. Roy. Statist. Soc. Ser. A* **143** 109–140.
- [6] BRU, M. F. (1989). Processus de Wishart. *C. R. Acad. Sci. Paris Sér. I Math.* **A308** 29–52.
- [7] CARNE, T. K. (1990). The geometry of shape spaces. *Proc. London Math. Soc.* (3) **61** 407–432.
- [8] CARNE, T. K. (1993). Maps from abuttals. Unpublished manuscript.
- [9] DIEUDONNÉ, J. (1970–4). *Treatise on Analysis, II–IV*. Academic, New York.
- [10] DRYDEN, I. L. (1989). The statistical analysis of shape data. Ph.D. dissertation, Univ. Leeds.
- [11] DRYDEN, I. L. and MARDIA, K. V. (1991). General shape distributions in a plane. *Adv. in Appl. Probab.* **23** 259–276.
- [12] GALLOT, S., HULIN, D. and LAFONTAINE, J. (1987). *Riemannian Geometry*. Springer, Berlin.
- [13] GOODALL, C. (1991). Procrustes methods in the statistical analysis of shape (with discussion). *J. Roy. Statist. Soc. Ser. B* **53** 285–339.
- [14] GOODALL, C. and MARDIA, K. V. (1992). The non-central Bartlett decomposition, and shape densities. *J. Multivariate Anal.* **40** 94–108.
- [15] GOODALL, C. and MARDIA, K. V. (1991). A geometrical derivation of the shape density. *Adv. in Appl. Probab.* **23** 496–514.
- [16] HELGASON, S. (1978–1984). *Differential Geometry, Lie Groups, and Symmetric Spaces and Groups and Geometric Analysis*. Academic, New York.
- [17] HERMANN, R. (1960). A sufficient condition that a mapping of Riemannian manifolds be a fibre bundle. *Proc. Amer. Math. Soc.* **11** 236–242.

- [18] HERMANN, R. (1960). On the differential geometry of foliations. *Ann. of Math.* **72** 445–457.
- [19] HILL, M. O. (1974). Correspondence analysis: A neglected multivariate method. *J. Roy. Statist. Soc. Ser. C* **23** 340–355.
- [20] ICKE, V. and VAN DE WEYGAERT, R. (1987). Fragmenting the universe, I. Statistics of 2-dimensional Voronoi foams. *Astronom. and Astrophys.* **184** 16–32. (See also [66] below.)
- [21] KENDALL, D. G. (1971). Construction of maps from “odd bits of information.” *Nature* **231** 158–159.
- [22] KENDALL, D. G. (1971). Maps from marriages. In *Mathematics in the Archaeological and Historical Sciences* (F. R. Hodson, D. G. Kendall and P. Tautu, eds.) Edinburgh Univ. Press.
- [23] KENDALL, D. G. (1975). The recovery of structure from fragmentary information. *Philos. Trans. Roy. Soc. London Ser. A* **279** 547–582.
- [24] KENDALL, D. G. (1977). The diffusion of shape. *Adv. in Appl. Probab.* **9** 428–430.
- [25] KENDALL, D. G. (1983). The shape of Poisson–Delaunay triangles. In *Papers in Honour of Octav Onicescu on his 90th Birthday* (M. C. Demetrescu and M. Iosifescu, eds.) 321–330. Nagard, Rome.
- [26] KENDALL, D. G. (1984). Shape manifolds, procrustean metrics, and complex projective spaces. *Bull. London Math. Soc.* **16** 81–121. (The reference to “local sections” on page 90 should be deleted.)
- [27] KENDALL, D. G. (1985). Exact distributions for shapes of random triangles in convex sets. *Adv. in Appl. Probab.* **17** 308–329.
- [28] KENDALL, D. G. (1986). Comment on “Size and shape spaces for landmark data in two dimensions” by F. L. Bookstein. *Statist. Sci.* **1** 222–226.
- [29] KENDALL, D. G. (1986). Further developments and applications of the statistical theory of shape. *Theory Probab. Appl.* **31** 407–412.
- [30] KENDALL, D. G. (1989). A survey of the statistical theory of shape (with discussion). *Statist. Sci.* **4** 87–120.
- [31] KENDALL, D. G. (1990). Random Delaunay simplexes in \mathbb{R}^m . *J. Statist. Plann. Inference* **25** 225–234.
- [32] KENDALL, D. G. (1991). The Mardia–Dryden shape distribution for triangles: a stochastic calculus approach. *J. Appl. Probab.* **28** 225–230.
- [33] KENDALL, D. G. (1991). Contribution to discussion following Goodall (1991).
- [34] KENDALL, D. G. (1992). Spherical triangles revisited. In *The Art of Statistical Science* (K. V. Mardia, ed.) 105–113. Wiley, Chichester.
- [35] KENDALL, D. G. (1993). Recovering the structure of a manorial estate from archival references. Unpublished manuscript.
- [36] KENDALL, D. G. (1993). The homology of the Euclidean shape spaces Σ_m^k . Unpublished manuscript.
- [37] KENDALL, D. G. and KENDALL, W. S. (1980). Alignments in 2-dimensional random sets of points. *Adv. in Appl. Probab.* **12** 380–424.
- [38] KENDALL, D. G. and LE, H. (1986). Exact distributions for shapes of random triangles in convex sets. *Adv. in Appl. Probab.* (Suppl.) 59–72.
- [39] KENDALL, D. G. and LE, H. (1987). The structure and explicit determination of convex-polygonally generated shape-densities. *Adv. in Appl. Probab.* **19** 896–916.
- [40] KENDALL, W. S. (1988). Symbolic computation and the diffusion of shapes of triads. *Adv. in Appl. Probab.* **20** 775–797.
- [41] KENDALL, W. S. (1990). The diffusion of Euclidean shape. In *Disorder in Physical Systems* (G. Grimmett and D. Welsh, eds.) Oxford Univ. Press.
- [42] KENT, J. T. (1992). New directions in shape analysis. In *The Art of Statistical Science* (K. V. Mardia, ed.) 115–127. Wiley, Chichester.
- [43] LE, H. (1987). Explicit formulae for polygonally generated shape densities in the basic tile. *Math. Proc. Cambridge Philos. Soc.* **101** 313–321.
- [44] LE, H. (1987). Singularities of convex-polygonally generated shape-densities. *Math. Proc. Cambridge Philos. Soc.* **102** 587–596.
- [45] LE, H. (1988). Shape theory in flat and curved spaces, and shape densities with uniform generators. Ph.D. dissertation, Univ. Cambridge.

- [46] LE, H. (1989). Random spherical triangles, I. Geometrical background. *Adv. in Appl. Probab.* **21** 570–580.
- [47] LE, H. (1989). Random spherical triangles, II. Shape densities. *Adv. in Appl. Probab.* **21** 581–594.
- [48] LE, H. (1990). A stochastic calculus approach to the shape distribution induced by a complex normal model. *Math. Proc. Cambridge Philos. Soc.* **109** 221–228.
- [49] LE, H. (1991). On geodesics in Euclidean shape spaces. *J. London Math. Soc.* **44** 360–372.
- [50] LE, H. (1992). The shapes of non-generic figures, and applications to collinearity testing. *Proc. Roy Soc. London Ser. A* **439** 197–210.
- [51] LE, H. (1993). Brownian motions on shape and size-and-shape spaces. *J. Appl. Probab.* To appear.
- [52] MARDIA, K. V. and DRYDEN, I. L. (1989). Shape distributions for landmark data. *Adv. in Appl. Probab.* **21** 742–755.
- [53] MARDIA, K. V. and DRYDEN, I. L. (1989). The statistical analysis of shape data. *Biometrika* **76** 271–281.
- [54] O'NEILL, B. (1966). The fundamental equations of a submersion. *Michigan Math. J.* **13** 459–469.
- [55] O'NEILL, B. (1967). Submersions and geodesics. *Duke Math. J.* **34** 363–373.
- [56] O'NEILL, B. (1983). *Semi-Riemannian Geometry*. Academic, New York.
- [57] REINHART, B. L. (1959). Foliated manifolds with bundle-like metrics. *Ann. of Math. (2)* **69** 119–132.
- [58] ROGERS, L. C. G. and WILLIAMS, D. (1987). *Diffusions, Markov Processes, and Martingales: Itô Calculus*. Wiley, Chichester.
- [59] ROHLF, F. J. and BOOKSTEIN, F. L., eds. (1990). *Proceedings of the Michigan Morphometrics Workshop*. Univ. Michigan Museum of Zoology, Special publication 2.
- [60] SMALL, C. G. (1981). Distribution of shape and maximal invariant statistics. Ph.D. dissertation, Univ. Cambridge.
- [61] SMALL, C. G. (1982). Random uniform triangles and the alignment problem. *Math. Proc. Cambridge Philos. Soc.* **91** 315–322.
- [62] SMALL, C. G. (1983). Characterisation of distributions from maximal invariant statistics. *Z. Wahrsch. Verw. Gebiete* **63** 517–527.
- [63] SMALL, C. G. (1984). A classification theorem for planar distributions based on the shape statistics of independent tetrads. *Math. Proc. Cambridge Philos. Soc.* **96** 543–547.
- [64] SMALL, C. G. (1988). Techniques of shape analysis on sets of points. *Internat. Statist. Rev.* **56** 243–257.
- [65] STOYAN, D., KENDALL, W. S. and MECKE, J. (1987). *Stochastic Geometry and Its Applications*. Wiley, Chichester.
- [66] VAN DE WEYGAERT, R. (1991). Voids and the geometry of large scale structure. Ph.D. dissertation, Rijksuniversiteit Leiden. (Cf. [20] above.)

DEPARTMENT OF MATHEMATICS
UNIVERSITY OF NOTTINGHAM
NOTTINGHAM NG7 2RD
UNITED KINGDOM

STATISTICAL LABORATORY
UNIVERSITY OF CAMBRIDGE
16 MILL LANE
CAMBRIDGE CB2 1SB
UNITED KINGDOM